

Gravitational collapse to extremal black holes and the third law of black hole thermodynamics

Christoph Kehle^{*1} and Ryan Unger^{†2}

¹*Institute for Theoretical Studies & Department of Mathematics, ETH Zürich,
Clausiusstrasse 47, 8092 Zürich, Switzerland*

²*Department of Mathematics, Princeton University,
Washington Road, Princeton NJ 08544, United States of America*

February 15, 2024

Abstract

We construct examples of black hole formation from regular, one-ended asymptotically flat Cauchy data for the Einstein–Maxwell-charged scalar field system in spherical symmetry which are exactly isometric to extremal Reissner–Nordström after a finite advanced time along the event horizon. Moreover, in each of these examples the apparent horizon of the black hole coincides with that of a Schwarzschild solution at earlier advanced times. In particular, our result can be viewed as a definitive *disproof* of the “third law of black hole thermodynamics.”

The main step in the construction is a novel C^k characteristic gluing procedure, which interpolates between a light cone in Minkowski space and a Reissner–Nordström event horizon with specified charge to mass ratio e/M . Our setup is inspired by the recent work of Aretakis–Czimek–Rodnianski on perturbative characteristic gluing for the Einstein vacuum equations. However, our construction is fundamentally nonperturbative and is based on a finite collection of scalar field pulses which are modulated by the Borsuk–Ulam theorem.

^{*}christoph.kehle@eth-its.ethz.ch

[†]runger@math.princeton.edu

Contents

1	Introduction	3
1.1	Event horizon gluing	5
1.2	Gravitational collapse from event horizon gluing	5
1.3	Characteristic gluing setup and proof	7
1.3.1	Previous work on characteristic gluing	7
1.3.2	Outline of the proof of Theorem 2	8
1.4	Retiring the third law of black hole thermodynamics	10
1.4.1	The singular massive dust shell model	10
1.4.2	The charged null dust model	11
1.4.3	“Losing trapped surfaces” and connectedness of the outermost apparent horizon	11
1.4.4	Disproving the third law	12
1.4.5	Exceptionality and stability of third law violating solutions	12
1.4.6	Aside: Extremal horizons with nearby trapped surfaces	13
1.5	Future boundary of the interior and Cauchy horizon gluing	14
1.5.1	Future boundary of the interior in Theorem 1	14
1.5.2	Gravitational collapse with a piece of smooth Cauchy horizon	14
1.5.3	Black hole interiors for which the Cauchy horizon closes off spacetime	15
2	The characteristic initial value problem for the Einstein–Maxwell-charged scalar field system in spherical symmetry	16
2.1	The Einstein–Maxwell-charged scalar field system in spherical symmetry	16
2.1.1	Spherically symmetric spacetimes	16
2.1.2	The Einstein–Maxwell-charged scalar field system	17
2.2	The characteristic initial value problem	18
2.2.1	Bifurcate characteristic data	18
2.2.2	Determining transversal derivatives from tangential data	19
2.3	Sphere data and cone data	19
2.3.1	Sphere data	19
2.3.2	Cone data and seed data	21
3	The main gluing theorems	21
3.1	Characteristic gluing in spherical symmetry	21
3.2	Spacetime gluing from characteristic gluing	22
3.3	Sphere data in Minkowski, Schwarzschild, and Reissner–Nordström	24
3.4	Main gluing theorems	25
4	Proofs of the main gluing theorems	26
4.1	Proof of Theorem 2A	27
4.2	Proof of Theorem 2B	29
4.3	Proof of Theorem 2C	34
5	Constructing the spacetimes and Cauchy data	35
5.1	Maximal future developments of asymptotically flat data for EMCSF	36
5.2	Construction of gravitational collapse to Reissner–Nordström	37
5.3	Construction of counterexample to the third law	39
5.4	Construction of collapse to Reissner–Nordström with piece of Cauchy horizon	41
5.5	Construction of black hole interior for which the Cauchy horizon closes off spacetime	42
A	An isolated extremal horizon with nearby trapped surfaces	43
B	General trapped and antitrapped surfaces in spherically symmetric spacetimes	44
	References	46

1 Introduction

Following pioneering work of Christodoulou [Chr70] and Hawking [Haw71] on energy extraction from rotating black holes, Bardeen, Carter, and Hawking [BCH73] proposed—via analogy to classical thermodynamics—the celebrated *four laws of black hole thermodynamics*. In particular, letting the surface gravity κ of the black hole take the role of its temperature, an identification later vindicated by the discovery of Hawking radiation [Haw75], they proposed a *third law* in analogy to “Nernst’s theorem” in classical thermodynamics.

Conjecture (The third law of black hole thermodynamics). *A subextremal black hole cannot become extremal in finite time by any continuous process, no matter how idealized, in which the spacetime and matter fields remain regular and obey the weak energy condition.*

This version is distilled from the literature, particularly from the work of Israel [Isr86; Isr92] who added explicit mention of regularity and the weak energy condition to avoid previously known examples [DI67; Kuc68; Bou73; FH79; SI80; Pr683] which would otherwise violate the third law. In this paper, we show that the third law is fundamentally flawed in a manner that does not appear to be salvageable by further reformulation. Indeed, we construct counterexamples in the Einstein–Maxwell-charged scalar field model in spherical symmetry, a model which satisfies the dominant energy condition, arising from arbitrarily regular initial data on a one-ended asymptotically flat hypersurface.

Theorem 1. *Subextremal black holes can become extremal in finite time, evolving from regular initial data. In fact, there exist regular one-ended Cauchy data for the Einstein–Maxwell-charged scalar field system which undergo gravitational collapse and form an exactly Schwarzschild apparent horizon, only for the spacetime to form an exactly extremal Reissner–Nordström event horizon at a later advanced time.*

In particular, the “third law of black hole thermodynamics” is false.

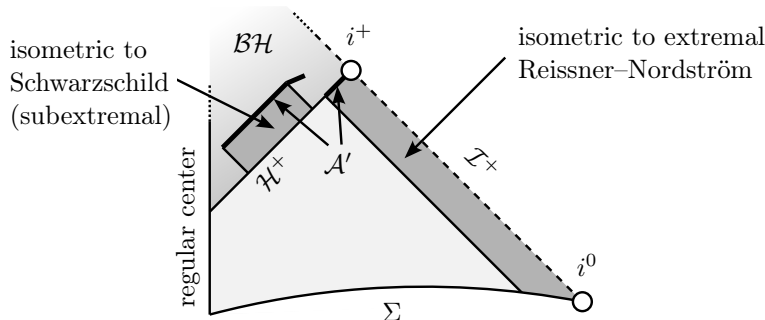


Figure 1: Penrose diagram of our counterexample to the third law arising from regular initial data on Σ . The northwest edge of the Schwarzschild region is exactly isometric to a section of the $r = 2M$ hypersurface in Schwarzschild. The outermost apparent horizon \mathcal{A}' is initially indistinguishable from Schwarzschild and then jumps out in finite time to be exactly isometric to the event horizon of extremal Reissner–Nordström. For speculations about the future boundary of the interior, see already Section 1.5.1. The behavior of our solutions can be modified to be subextremal near i^0 , see already Remark 1.1.

Our result also clarifies some issues raised by Israel in [Isr86; Isr92] who seemingly associated a disconnected outermost apparent horizon with a severe lack of regularity of the spacetime metric and/or matter fields. We stress that our examples are regular despite the disconnectedness of the apparent horizon. We note moreover that Israel seemed to associate extremization with the black hole “losing its trapped surfaces.” This confusion appears to be related to his implicit assumption that the apparent horizon is connected. Since the Einstein–Maxwell-charged scalar field matter manifestly obeys the dominant energy condition, trapped surfaces are not lost in any sense, nonetheless, the black hole becomes extremal in finite time. In the examples we construct, there exists an open set of trapped spheres inside the black hole region, which persist for all advanced time until they encounter the Cauchy horizon or a curvature singularity inside the black hole. However, there is a neighborhood of the event horizon which does not contain any (strictly) trapped surfaces. For an extended discussion of these issues, see already Section 1.4.

Remark 1.1. Note that in discussions of the third law, the focus is typically on dynamics near the event horizon and apparent horizon, in late advanced time. Our counterexamples depicted in Fig. 1 are isometric to extremal Reissner–Nordström for all sufficiently late advanced times and all retarded times to the past of the event horizon, in particular near spatial infinity i^0 . However, by using a scattering argument as in [Keh22], one can easily modify our examples so as to be subextremal in a neighborhood of i^0 , if desired.

Our falsification of the third law (Theorem 1) is preceded by our following more general result. We construct regular one-ended Cauchy data for the Einstein–Maxwell-charged scalar field system in spherical symmetry whose black hole exterior evolves (in fact is eventually isometric) to a Schwarzschild black hole with prescribed mass $M > 0$ or to a *subextremal* or *extremal* Reissner–Nordström black hole with prescribed mass $M > 0$ and prescribed charge to mass ratio $q \doteq e/M \in [-1, 1]$. The Einstein–Maxwell-charged scalar field (EMCSF) system reads

$$R_{\mu\nu}(g) - \frac{1}{2}R(g)g_{\mu\nu} = 2(T_{\mu\nu}^{\text{EM}} + T_{\mu\nu}^{\text{CSF}}), \quad (1.1)$$

$$\nabla^\mu F_{\mu\nu} = 2\epsilon \text{Im}(\phi \overline{D_\nu \phi}), \quad (1.2)$$

$$g^{\mu\nu} D_\mu D_\nu \phi = 0, \quad (1.3)$$

for a quintuplet $(\mathcal{M}, g, F, A, \phi)$, where (\mathcal{M}, g) is a (3+1)-dimensional Lorentzian manifold, ϕ is a complex-valued scalar field, A is a real-valued 1-form, $F = dA$ is a real-valued 2-form, $D = d + i\epsilon A$ is the gauge covariant derivative, $\epsilon \in \mathbb{R} \setminus \{0\}$ is a fixed coupling constant representing the charge of the scalar field, and the energy momentum tensors are defined by

$$T_{\mu\nu}^{\text{EM}} \doteq g^{\alpha\beta} F_{\alpha\nu} F_{\beta\mu} - \frac{1}{4} F^{\alpha\beta} F_{\alpha\beta} g_{\mu\nu}, \quad (1.4)$$

$$T_{\mu\nu}^{\text{CSF}} \doteq \text{Re}(D_\mu \phi \overline{D_\nu \phi}) - \frac{1}{2} g_{\mu\nu} g^{\alpha\beta} D_\alpha \phi \overline{D_\beta \phi}. \quad (1.5)$$

We refer to Section 2 for the form of the EMCSF system in spherical symmetry.

Remark 1.2. All of the results in this paper also hold for the *Einstein–Maxwell–charged Klein–Gordon* system in which the wave equation (1.3) is replaced by the Klein–Gordon equation

$$g^{\mu\nu} D_\mu D_\nu \phi = m^2 \phi,$$

where $m \in \mathbb{R}_{>0}$ represents the mass of the scalar field and satisfies $mM \ll \epsilon M$. Here M denotes the mass of the black holes, see already Theorem 2 below.

We emphasize that not only are our data in the above examples regular, but the spacetimes arise from gravitational collapse, i.e., the initial data surface is one-ended, has a regular center, lies entirely in the domain of outer communication, and the black hole forms strictly to the future of initial data. In particular, in contrast to what has been suggested numerically [TA14; CIP21], there is no upper bound (strictly less than unity) on the charge to mass ratio of a black hole which can be achieved in gravitational collapse for this model.

The key step toward the construction of one-ended Cauchy data evolving to black holes with prescribed mass and charge is a novel *characteristic/null gluing* result. The study of the characteristic gluing problem for the Einstein vacuum equations (outside of spherical symmetry) was recently initiated by Aretakis, Cizmek, and Rodnianski [ACR21a; ACR21b; ACR21c] in the perturbative regime around Minkowski space. Our setup is directly inspired by their work. In contrast, however, our null gluing construction (while in spherical symmetry) necessarily exploits the *large data regime* in order to glue a cone of Minkowski space to a black hole event horizon along a null hypersurface within the EMCSF model. The construction of Cauchy data on $\Sigma \cong \mathbb{R}^3$ collapsing to an extremal or subextremal event horizon will then follow from Theorem 2 as Corollary 1 presented in Section 1.2.

On the basis of our spherically symmetric horizon gluing construction in Theorem 2, the results and framework introduced in [ACR21a; ACR21b; ACR21c; CR22; DHR], and Remark 1.5 below, we formulate the following

Conjecture. *There exist regular one-ended Cauchy data for the Einstein vacuum equations*

$$\text{Ric}(g) = 0$$

which undergo gravitational collapse and form an exactly Schwarzschild apparent horizon, only for the space-time to form an exactly extremal Kerr event horizon at a later advanced time. In particular, already in vacuum, the “third law of black hole thermodynamics” is false.

1.1 Event horizon gluing

We will now state the rough version of our main null gluing theorem, which concerns gluing a null cone in Minkowski space to a Reissner–Nordström event horizon.

Theorem 2 (Rough version). *Let $k \in \mathbb{N}$ be a regularity index, $q \in [-1, 1]$ a charge to mass ratio, and $\epsilon \in \mathbb{R} \setminus \{0\}$ a fixed coupling constant. For any M sufficiently large depending on k , q , and ϵ , there exist spherically symmetric characteristic data for the Einstein–Maxwell-charged scalar field system with coupling constant ϵ gluing a Minkowski null cone of radius $\frac{1}{2}M$ to a Reissner–Nordström event horizon with mass M and charge $e = qM$ up to order k .*

We also refer to Fig. 2 for an illustration of our construction.

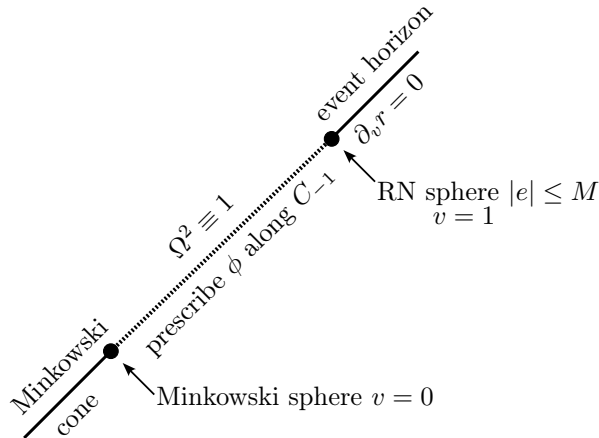


Figure 2: Setup of Theorem 2.

For the precise version of Theorem 2 we refer to Theorem 2A and Theorem 2B in Section 3.4. In fact, more generally, we can replace the Minkowski sphere with certain Schwarzschild exterior spheres at $v = 0$, which is important for constructing counterexamples to the third law of black hole thermodynamics (see already Section 1.4). Furthermore, when $q = 0$ we may take the scalar field to be real-valued, in which case the EMCSF system collapses to the Einstein-scalar field system.

Remark 1.3. For the proofs of Corollary 2 and Corollary 3 below, we will use versions of Theorem 2 where the top sphere is not located on a horizon. See Theorem 2C and Theorem 2C' in Section 3.4 below.

Remark 1.4. With our methods one can also construct characteristic data which are exactly Minkowski initially and then settle down, but only asymptotically, to a Schwarzschild or (sub-)extremal Reissner–Nordström event horizon of prescribed mass and charge. The rate of decay can be chosen to be $|\partial_v \phi| \approx v^{-p}$, $p > \frac{1}{2}$, in a standard Eddington–Finkelstein gauge for Schwarzschild or subextremal Reissner–Nordström black holes. This provides examples of “global” characteristic data settling down at certain prescribed rates as assumed in [Van18; GL19; KV21].

1.2 Gravitational collapse from event horizon gluing

For appropriate matter models, the Einstein equations

$$\text{Ric}(g) - \frac{1}{2}R(g)g = 2T$$

are well-posed (see [Fou52; CG69] for the vacuum case) as a Cauchy problem for suitable initial data posed on a 3-manifold Σ , which will then be isometrically embedded as a spacelike hypersurface in a Lorentzian manifold (\mathcal{M}, g) . The textbook explicit black hole solutions such as the Schwarzschild spacetime do not contain *one-ended* Cauchy surfaces $\Sigma \cong \mathbb{R}^3$ but are instead foliated by *two-ended* hypersurfaces $\Sigma \cong \mathbb{R} \times S^2$. Thus, a natural and physically relevant problem is to construct regular asymptotically flat data on $\Sigma \cong \mathbb{R}^3$ which evolve to a black hole spacetime. The first example of *gravitational collapse*, that is a black hole

spacetime containing a one-ended Cauchy surface which lies outside of the black hole region, was constructed by Oppenheimer and Snyder [OS39] for the Einstein-massive dust model in spherical symmetry.

Using Theorem 2, by solving the Einstein equations *backwards*, we construct examples of gravitational collapse where the domain of outer communication is eventually exactly isometric to Reissner–Nordström with prescribed mass and charge. The proof of the following Corollary 1 is given in Section 5.2.

Corollary 1 (Exact Reissner–Nordström arising from gravitational collapse). *For any regularity index $k \in \mathbb{N}$ and charge to mass ratio $q \in [-1, 1]$, there exist spherically symmetric, asymptotically flat Cauchy data for the Einstein–Maxwell-charged scalar field system, with $\Sigma \cong \mathbb{R}^3$ and a regular center, such that the maximal future globally hyperbolic development (\mathcal{M}^4, g) has the following properties:*

- All dynamical quantities are at least C^k -regular.
- Null infinity \mathcal{I}^+ is complete.
- The black hole region is non-empty, $\mathcal{BH} \doteq \mathcal{M} \setminus J^-(\mathcal{I}^+) \neq \emptyset$.
- The Cauchy surface Σ lies in the causal past of future null infinity, $\Sigma \subset J^-(\mathcal{I}^+)$. In particular, Σ does not intersect the event horizon $\mathcal{H}^+ \doteq \partial(\mathcal{BH})$. Furthermore, Σ contains no trapped or antitrapped surfaces.
- For sufficiently late advanced times $v \geq v_0$, the domain of outer communication, including the event horizon, is isometric to that of a Reissner–Nordström solution with charge to mass ratio q . For $v \geq v_0$, the event horizon of the spacetime can be identified with the event horizon of Reissner–Nordström.

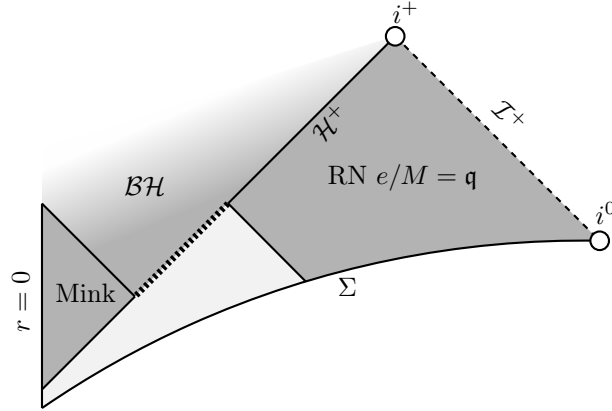


Figure 3: Penrose diagram for Corollary 1. The textured line segment is where the data constructed in Theorem 2 live.

Note that in the case $|q| = 1$, this does not yet furnish a counterexample to the third law of black hole thermodynamics, as the spacetime does not necessarily contain a subextremal apparent horizon. For the counterexample we must defer to Theorem 1 in Section 1.4.4 below.

However, in our proof of Corollary 1, forming an extremal black hole with $|q| = 1$ is no different from any subextremal charge to mass ratio $|q| < 1$ (see already Section 1.4.5). In particular, in contrast with what has been suggested by numerical simulations [TA14; CIP21], there is no universal upper bound (strictly less than unity) for $|q|$. Given that we have now proved that extremal Reissner–Nordström can arise in gravitational collapse, it would be interesting to rethink the numerical approach to this problem and develop a scheme to construct such solutions numerically. Because our construction is fundamentally teleological (see already Section 5.1), it might be challenging to directly find suitable data on Σ by trial and error.

The formation of black holes is a very well studied problem in spherical symmetry. We mention here only the Einstein-scalar field model, for which Christodoulou [Chr91] first showed that concentration of the scalar field can lead to formation of a black hole. This result played a decisive role in Christodoulou’s proof of weak cosmic censorship in spherical symmetry [Chr99]. Dafermos constructed solutions of the Einstein-scalar field

system which collapse to the future but are complete and regular to the past [Daf09]. For work on other matter models, see for example [And14; AL22].

Outside of spherical symmetry (for the Einstein vacuum equations), formation of black holes was studied by Christodoulou in the seminal monograph [Chr09]. Christodoulou constructed *characteristic data* for the Einstein vacuum equations containing no trapped surfaces, but whose evolution contains trapped surfaces in the future. Li and Yu [LY15] showed how to combine Christodoulou’s construction with the spacelike gluing technique of Corvino and Schoen [CS06] to construct asymptotically flat *Cauchy data* containing no trapped surfaces, but whose evolution contains trapped surfaces in the future. Later, Li and Mei [LM20] observed that the Corvino–Schoen gluing can be done “behind the event horizon,” which yields a genuine construction of gravitational collapse in vacuum arising from one-ended asymptotically flat Cauchy data.

However, the constructions of the above type rely on the observation that if an additional restriction is imposed on the seed data in [Chr09], then the resulting spacetime has a region of controlled size which is close to Schwarzschild. The Corvino–Schoen gluing then selects *very slowly rotating* Kerr parameters for the exterior region.

We emphasize that our gluing approach yields collapsing spacetimes with exactly specified (in particular, extremal, if desired) parameters, but is so far limited to spherical symmetry.

Remark 1.5. Our derivation of Corollary 1 from Theorem 2 is completely soft and does not make use of spherical symmetry. Therefore, if versions of the main gluing theorems were known for the Einstein vacuum equations (for example, gluing a Minkowski cone to an extremal Kerr event horizon, or more generally a Schwarzschild exterior sphere to an extremal Kerr event horizon), then our procedure would yield vacuum spacetimes arising from gravitational collapse which are eventually isometric to extremal Kerr. Furthermore, such a construction would also yield a disproof of the third law in vacuum.

Remark 1.6. By the very nature of our gluing procedure, the constructions in this paper have finite regularity (C^k for arbitrarily large k). It would be mathematically interesting to create such examples with C^∞ regularity. See already Remark 1.8.

Remark 1.7. The existence of dynamical spacetimes satisfying the dominant energy condition which are extremal at spacelike infinity i^0 does not contradict the positive mass theorem “with charge” [GHHP83; CRT06] because the matter itself carries charge. Concretely, condition (27) in [GHHP83] is false for various charged matter models, in particular the Einstein–Maxwell-charged scalar field model with small (or zero) mass.

1.3 Characteristic gluing setup and proof

1.3.1 Previous work on characteristic gluing

The gluing problem along characteristic hypersurfaces for hyperbolic equations and associated null constraints already appears for the linear wave equation on Minkowski space. On \mathbb{R}^{3+1} , let $u = \frac{1}{2}(t - r)$, $v = \frac{1}{2}(t + r)$, and let ϕ be a spherically symmetric solution to the wave equation, i.e.,

$$\partial_u \partial_v (r\phi) = 0. \tag{1.6}$$

Let $C \cup \underline{C}$ be a spherically symmetric bifurcate null hypersurface, that is, $C = \{u = u_0\} \cap \{v \geq v_0\}$ and $\underline{C} = \{u_1 \geq u \geq u_0\} \cap \{v = v_0\}$. The wave equation (1.6) implies that $\partial_u(r\phi)$ is *conserved along the outgoing cone* C . This implies that $\partial_u \phi$ cannot be freely prescribed along C , but is in fact determined by $\partial_u \phi$ on the bifurcation sphere $C \cap \underline{C}$. Indeed, the characteristic initial value problem is well posed with just ϕ itself prescribed along $C \cup \underline{C}$ —the full 1-jet of ϕ can then be recovered from (1.6). For general spacetimes, the question of null gluing for the linear wave equation was studied by Aretakis [Are17].

For a general wave equation, ingoing derivatives satisfy transport equations along outgoing null cones. The general C^k characteristic gluing problem is to be given two spheres S_1 and S_2 along an outgoing null cone C , and k ingoing and outgoing derivatives of ϕ at S_1 and S_2 . One then seeks to prescribe ϕ along the part of C between S_1 and S_2 so that the outgoing derivatives agree with the given ones and the solutions of the transport equations for the ingoing derivatives have the specified initial and final values. In general, the linear characteristic gluing problem is obstructed due to the presence of *conserved charges* stemming from *conservation laws* along C .

Remark 1.8. Even in the absence of conservation laws at any order, C^∞ gluing of transverse derivatives may be obstructed in linear theory. This can be seen already for the $(1+1)$ -dimensional wave equation $\partial_u \partial_v \phi = f(u, v)\phi$ for generic $f \in C^\infty(\mathbb{R}^{1+1})$. For such an f , there are no conservation laws at any order and by imposing trivial data at S_1 and very rapidly growing (in k) ∂_u^k -derivatives at S_2 , one can show that C^∞ gluing cannot be achieved. Note that in $1+1$ dimensions, S_1 and S_2 are points.

The null gluing problem for the Einstein vacuum equations was recently initiated by Aretakis, Czimek, and Rodnianski in a fundamental series of papers [ACR21a; ACR21b; ACR21c]. Their proof uses the inverse function theorem to reduce the nonlinear problem to a linear characteristic gluing problem for the linearized Einstein equations in double null gauge around Minkowski space, in the formalism of Dafermos–Holzegel–Rodnianski [DHR]. This linearized problem is carefully analyzed and the authors identify *infinitely many* conserved charges which are obstructions to the linear gluing problem. All but ten of the charges turn out to be related to linearized gauge transformations (cf. the “pure gauge solutions” of [DHR]). An inverse function theorem argument then gives nonlinear gluing close to Minkowski space, provided that, *a posteriori*, the 10 transported gauge-invariant charges at S_2 agree with the prescribed charges on S_2 (which is in fact also perturbed to deal with the gauge-dependent charges). Very recently, Czimek and Rodnianski [CR22] carefully exploited the *nonlinear* structure of the null constraint equations to nonlinearly compensate for failure of matching of the linearly conserved charges. In this way, the authors prove obstruction-free gluing for characteristic and Cauchy data near Minkowski space.

In the present paper, we are however interested in a different regime of gluing. We wish to glue two specific null cones: a light cone in Minkowski space and a Reissner–Nordström event horizon, as a solution of the EMCSF null constraint system. On the one hand, this is a genuine “large data” gluing problem, as these cones are very dissimilar in a gauge invariant sense and there is no known spacetime around which one could reasonably linearize the equations. On the other hand, we study our problem in spherical symmetry, which makes it considerably more tractable. We refer to Section 3.1 below for a precise definition of characteristic gluing in spherical symmetry.

1.3.2 Outline of the proof of Theorem 2

In the Einstein–Maxwell-charged scalar field model in spherical symmetry, the spacetime metric is written in double null gauge as

$$g = -\Omega^2 du dv + r^2 g_{S^2},$$

where Ω^2 is the lapse and r the area-radius. We also have a complex-valued scalar field ϕ and a real-valued charge Q , which is related to the only nonzero component of the electromagnetic tensor F . We choose an electromagnetic gauge in which $A = A_u du$, where A is a gauge potential for F . The dynamical variables to be glued along an outgoing cone (which we will call $C_{-1} \doteq \{u = -1\}$) are $(r, \Omega^2, \phi, Q, A_u)$. The charge Q solves first order equations in u and v , A_u is computed from Q via $F = dA$, and the variables r , Ω^2 , and ϕ solve coupled nonlinear wave equations involving also Q and A_u . See already equations (2.4)–(2.9). Since the value of Ω^2 along any given null cone (or bifurcate null hypersurface) can be adjusted by reparametrizing the double null gauge, we impose that $\Omega^2 \equiv 1$.

We first consider *Raychaudhuri’s equation* (see already (2.11)), which reads in the gauge $\Omega^2 \equiv 1$

$$\partial_v^2 r = -r |\partial_v \phi|^2. \tag{1.7}$$

This equation gives a nonlinear constraint on C_{-1} and completely determines r on C_{-1} given r and $\partial_v r$ at one point of C_{-1} and ϕ along C_{-1} . Thus, in the gauge $\Omega^2 \equiv 1$ along C_{-1} , up to specifying the dynamical quantities at a sphere, the free data in this problem is exactly ϕ on C_{-1} : All other dynamical quantities and their derivatives (both in the u and v coordinates) along C_{-1} can be obtained from ϕ and the equations (2.4)–(2.11).

We will choose ϕ to be compactly supported on the textured segment in Fig. 2 and set

$$\partial_u \phi(0) = \cdots = \partial_u^k \phi(0) = 0,$$

where k is the order at which we wish to glue. A first attempt to solve the gluing problem would be to set (r, Ω^2, Q, A_u) and derivatives to have their “Minkowski values” at the sphere $v = 0$ and then prescribe $\phi(v)$ so that the dynamical variables reach their “Reissner–Nordström values” at $v = 1$. However, specifying

a “Minkowski value” for $\partial_v r$ is essentially another gauge choice, and the gauge invariance of the equations enables a much more convenient strategy.

Given that ϕ vanishes to order k at $v = 0$, to know that the sphere $v = 0$ is a sphere in Minkowski space to order k , we merely need to know that $r(0) > 0$ and that the charge Q and the Hawking mass (see already (2.1)) both vanish. See already Lemma 4.1. This reduces to the statement that in the gauge $\Omega^2 \equiv 1$,

$$\partial_u r(0) \partial_v r(0) = -\frac{1}{4}.$$

Since r solves a wave equation (see already (2.5)), $\partial_u r$ solves a first order equation in v , so it is determined on C_{-1} by $\partial_u r(0)$ alone. Given ϕ , we solve Raychaudhuri’s equation (1.7) *backwards*, i.e., we teleologically normalize r at the final sphere by setting

$$\begin{aligned} r(1) &= r_+ \doteq \left(1 + \sqrt{1 - \mathfrak{q}^2}\right) M \\ \partial_v r(1) &= 0 \end{aligned}$$

and then set

$$\partial_u r(0) \doteq \frac{-\frac{1}{4}}{\partial_v r(0)}.$$

Therefore the only “constraint” is that $\partial_v r(0) > 0$, which will be automatically satisfied by the monotonicity property of Raychaudhuri’s equation as long as $r > 0$.

The charge Q is determined by *Maxwell’s equation* (see already (2.8))

$$\partial_v Q = \epsilon r^2 \text{Im}(\phi \overline{\partial_v \phi}).$$

Integrating this forwards in v yields the charge condition

$$\int_0^1 \epsilon r^2 \text{Im}(\phi \overline{\partial_v \phi}) dv = \mathfrak{q} M. \quad (1.8)$$

At this point we note that if $r(0) \geq \frac{1}{2}M$, then the left-hand side of this equation is $\approx M^2 \int \text{Im}(\phi \overline{\partial_v \phi})$. So by modulating $\int \text{Im}(\phi \overline{\partial_v \phi})$, we can hope to satisfy this equation just on the basis of scaling ϕ itself.

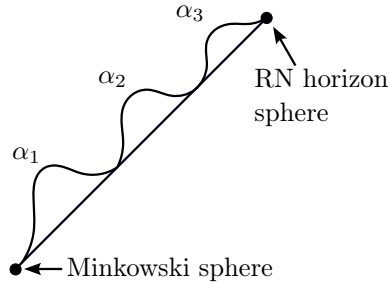


Figure 4: Schematic illustration of the pulses.

Our ansatz for the scalar field will be

$$\phi_\alpha = \sum_{1 \leq j \leq 2k+1} \alpha_j \phi_j,$$

where $\alpha = (\alpha_1, \dots, \alpha_{2k+1}) \in \mathbb{R}^{2k+1}$ and the ϕ_j ’s are smooth compactly supported complex-valued functions with disjoint supports. We assume $\mathfrak{q} \neq 0$ now, the $\mathfrak{q} = 0$ case being in fact much easier. The charge condition (1.8) is examined on every ray $\mathbb{R}_+ \hat{\alpha} \in \mathbb{R}^{2k+1}$, $\hat{\alpha} \in S^{2k}$. We show that for a given choice of baseline profiles ϕ_j , there is a smooth starshaped hypersurface $\mathfrak{Q}^{2k} \subset \mathbb{R}^{2k+1}$ which is isotopic to the unit sphere S^{2k} and invariant under the antipodal map $\alpha \mapsto -\alpha$ such that (1.8) holds for every $\alpha \in \mathfrak{Q}^{2k}$.

The condition that M is large depending on k , \mathfrak{q} , and ϵ in Theorem 2 comes from natural conditions that arise when attempting to construct the hypersurface \mathfrak{Q}^{2k} . The charge condition (1.8) implies $|\epsilon| M^2 |\alpha|^2 \approx$

$|q|M$ on \mathfrak{Q}^{2k} . However, to keep $r \geq \frac{1}{2}M$ on C_{-1} , we find the condition $|\alpha| \lesssim 1$, see already Lemma 4.4. These conditions are consistent only if $|\mathfrak{e}|M \gtrsim |q|$. Furthermore, this condition is crucially used to propagate the condition $\partial_u r < 0$, see already Lemma 4.8.

The remaining equations ($2k$ real equations since the scalar field is complex)

$$\partial_u^i \phi_\alpha(1) = 0 \quad 1 \leq i \leq k \quad (1.9)$$

can naturally be viewed as *odd* equations as a function of α . So when restricted to $\alpha \in \mathfrak{Q}^{2k}$, we can use the classical Borsuk–Ulam theorem to find a simultaneous solution. Once we have an $\alpha \in \mathfrak{Q}^{2k}$ such that (1.9) is satisfied, ϕ_α will glue all relevant quantities to k -th order, as desired.

Theorem 3 (Borsuk–Ulam [Bor33]). *If $f : S^k \rightarrow \mathbb{R}^k$ is a continuous odd function, i.e., $f(-x) = -f(x)$ for every $x \in S^k$, then f has a root.*

For a nice proof using only basic degree theory and transversality arguments, see Nirenberg’s lecture notes [Nir01].

1.4 Retiring the third law of black hole thermodynamics

In this section we give more details on the background and history of the third law of black hole thermodynamics put forth by Bardeen, Carter, and Hawking in [BCH73], and how our present work fits into the picture.

While the *zeroth*, *first*, and *second* laws of black hole thermodynamics are by now well understood in the literature (see e.g. [Wal01]), the validity of the third law has been a source of debate up until today. In the original form of Bardeen–Carter–Hawking (BCH), in analogy to Nernst’s version of the third law of classical thermodynamics [Ner26]¹, it reads:

It is impossible by any procedure, no matter how idealized, to reduce κ to zero by a finite sequence of operations.

A number of arguably pathological (e.g. singular or energy condition violating) examples of extremal black hole formation were put forth in [Kuc68; DI67; Pr683; Bou73; FH79; SI80], which Israel [Isr86; Isr92] took into account to make the third law more precise:

A nonextremal black hole cannot become extremal (i.e., lose its trapped surfaces) at a finite advanced time in any continuous process in which the stress-energy tensor of accreted matter stays bounded and satisfies the weak energy condition in a neighborhood of the outer apparent horizon.

The parenthetical comment “(i.e., lose its trapped surfaces)” is an extra source of confusion which will be specifically addressed in Section 1.4.3. We will now discuss the papers [Kuc68; DI67; Pr683; Bou73; FH79; SI80; Isr86; Isr92] and where the issues lie.

1.4.1 The singular massive dust shell model

It has been known since the 60’s that an extremal black hole can be formed instantly by collapsing an infinitesimally thin shell of charged massive dust [Kuc68; DI67; Pr683; Bou73]. Later, Farrugia and Hajicek [FH79] showed how to “turn a subextremal Reissner–Nordström spacetime into an extremal one” by firing an appropriately charged singular massive shell into the black hole. The resulting spacetime metric is not C^2 -regular. The Penrose diagram of the spacetime they construct is similar to our Fig. 1 (see [FH79, p. 296 Fig. 2]). In particular, we note the presence of a disconnected outermost apparent horizon in their example. Israel seemed to associate the disconnectedness of the apparent horizon with a singularity of the matter and/or spacetime: “Violations can also be produced by any process that induces discontinuous behavior of the apparent horizon—for example, absorption of an infinitely thin massive shell, which will force this horizon to jump outward.” See already Section 1.4.3. On the basis of this, he dismissed this example in his formulation of the third law by explicitly requiring regularity. We note, however, that Farrugia and Hajicek suggest that their construction can in principle be desingularized—we do not know if this point was ever addressed again, because if true, it would seem to provide an alternative route to constructing a counterexample apart from our own.

¹For a discussion of various versions of the third law of classical thermodynamics, see [Wal97].

1.4.2 The charged null dust model

An interesting example motivating explicit mention of the weak energy condition in the third law was provided by Sullivan and Israel [SI80] in spherical symmetry, with the charged null dust matter model. This matter model allows for *dynamical* violations of the weak energy condition—even if the initial data satisfies the weak energy condition, the solution might violate it in the future. Sullivan and Israel showed that extremization is impossible in this model without such a violation, which can also be seen from Penrose diagrams. They interpreted this result as further evidence that the third law holds as long as the weak energy condition is demanded near the apparent horizon. We note, however, that Ori has proposed a different interpretation of the model studied by Sullivan and Israel which does not violate the weak energy condition [Ori91].

1.4.3 “Losing trapped surfaces” and connectedness of the outermost apparent horizon

We will now clarify the issue of “losing trapped surfaces” appearing prominently in [Isr86; Isr92] and the implicit assumption of connectedness of the outermost apparent horizon.

The black hole region in a subextremal Reissner–Nordström or Kerr spacetime is foliated by trapped spheres. Conversely, extremal Reissner–Nordström and Kerr black holes have no trapped surfaces, but the event horizon is a marginally trapped tube in both cases. As $|q| \rightarrow 1$ (where we take $q \doteq e/M$ for Reissner–Nordström and $q \doteq a/M$ for Kerr), $r_- \rightarrow r_+$, and one might be inclined to think that extremizing involves “squeezing” away the trapped region inside the black hole. However, it is an immediate consequence of Raychaudhuri’s equation [HE73; Wal84] that trapped surfaces persist in evolution as long as the spacetime satisfies the weak energy condition. Since the typical explicit extremal black holes have no trapped surfaces (in particular none near the event horizon), one might wonder if Raychaudhuri’s equation alone could be used to “prove” the third law.

This is what Israel attempted to do in [Isr86; Isr92]. We will formalize his observation in Definition 1.1 and Proposition 1.1 below. However, as should be clear from our main theorem, this does not in fact capture the intended meaning of the third law.

In order to reconstruct Israel’s argument mathematically, let us formulate the following definition. For precise definitions relating to spherical symmetry, see already Section 2.

Definition 1.1. Let H be a connected dynamical apparent horizon, i.e., a connected, achronal curve in the $(1+1)$ -dimensional reduction $(\mathcal{Q}, g_{\mathcal{Q}})$ of a spherically symmetric spacetime (\mathcal{M}, g) , along which $\partial_v r$ vanishes identically. We say that H *becomes extremal in finite time in the sense of Israel* if

1. H is not completely contained in a null cone.
2. Let $\tau \mapsto H(\tau)$ be a parametrization of H . Then there exists a $\tau_0 \in \mathbb{R}$ so that for all $\tau \geq \tau_0$, $\tau \mapsto H(\tau)$ is a future-directed constant u curve.
3. There exists a $\tau_1 > \tau_0$ and a neighborhood \mathcal{N} of $H_{\tau \geq \tau_1}$ such that $\mathcal{N} \setminus H_{\tau \geq \tau_0}$ contains only strictly untrapped spheres ($\partial_v r > 0$).

Remark 1.9. The outermost apparent horizon \mathcal{A}' (see already Section 5.1), if connected, is an example of a connected dynamical apparent horizon.

As a simple consequence of Raychaudhuri’s equation in a spacetime satisfying the weak energy condition [HE73; Wal84], we have

Proposition 1.1 (Israel’s observation). *Let (\mathcal{M}, g) be a spherically symmetric black hole spacetime. If the spacetime satisfies the weak energy condition, has a nonempty trapped region, and a connected outermost apparent horizon \mathcal{A}' as defined in [Kom13], then the outermost apparent horizon \mathcal{A}' does not become extremal in finite time in the sense of Israel.*

However, it is clear that in view of our main theorem, the correct reading of this proposition is the *contrapositive*, namely that violations of the third law necessarily have a disconnected apparent horizon. This effect has nothing to do with singularities of spacetime or the matter model (and there was never actually any *a priori* reason to believe that the outermost apparent horizon was connected). This situation is depicted in Fig. 5.

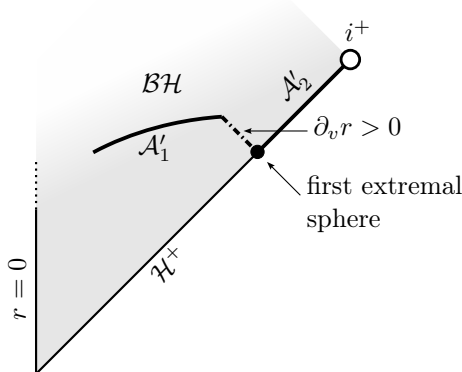


Figure 5: Illustration of the contrapositive of Proposition 1.1. The outermost apparent horizon $\mathcal{A}' = \mathcal{A}'_1 \cup \mathcal{A}'_2$ becomes disconnected when a black hole with trapped surfaces “becomes extremal,” while the spacetime and matter fields remain regular. The trapped region begins to the north of \mathcal{A}'_1 and persists for all advanced time.

1.4.4 Disproving the third law

With this discussion out of the way, we present now a detailed version of our counterexample to the third law. It is essentially a corollary of the more general version of our main gluing result Theorem 2 with a Schwarzschild exterior sphere in place of a Minkowski sphere (see already Section 3.4) and will be given in Section 5.3. For an illustration of the spacetime, we refer the reader back to Fig. 1.

Theorem 1 (Gravitational collapse to ERN with a Schwarzschild piece). *For any regularity index $k \in \mathbb{N}$, there exist spherically symmetric, asymptotically flat Cauchy data for the Einstein–Maxwell-charged scalar field system, with $\Sigma \cong \mathbb{R}^3$ and a regular center, such that the maximal future globally hyperbolic development (\mathcal{M}^4, g) has the following properties:*

- *The spacetime satisfies all the conclusions of Corollary 1 with $\mathfrak{q} = 1$, including C^k -regularity of all dynamical quantities.*
- *The black hole region contains an isometrically embedded portion of a Schwarzschild exterior horizon neighborhood. In particular, there is a portion of a null cone behind the event horizon of (\mathcal{M}, g) which can be identified with a portion of the apparent horizon of Schwarzschild.*
- *The “Schwarzschild horizon” piece is a part of the outermost apparent horizon \mathcal{A}' of the spacetime. The set \mathcal{A}' is disconnected and agrees with the event horizon \mathcal{H}^+ to the future of the first marginally trapped sphere on the event horizon.*
- *There is a neighborhood of the event horizon that contains no trapped surfaces. Nonetheless, the black hole region contains trapped surfaces. In fact, there are trapped surfaces at arbitrarily late advanced time in the interior of the black hole.*

To reiterate, the scalar field collapses to form an *exact* Schwarzschild spacetime, including the horizon, only to collapse further to form an *exact* extremal Reissner–Norström for all late advanced time. The spacetime is regular (for any fixed $k \geq 1$, one can construct an example which is C^k) and the matter model satisfies the dominant energy condition.

1.4.5 Exceptionality and stability of third law violating solutions

The third law is manifestly concerned with exceptional behavior, which is why the phrases “no matter how idealized” [BCH73] or “in any continuous process” [Isr86] are specifically included in formulations of the third law. Indeed, keeping a horizon at exactly constant temperature (or equivalently constant surface gravity), any temperature, is of course exceptional. (Exactly stationary behavior on the horizon for all late

advanced times is itself an infinite codimension phenomenon in the moduli space of solutions.) In view of our construction, the case of gravitational collapse to zero temperature in finite time is no more exceptional than any other fixed temperature.

We would also like to address the interesting question of whether creating *asymptotically* extremal black holes should be viewed any differently from the subextremal case. Indeed, any mechanism which forms a black hole with *exactly specified* parameters is inherently unstable, because a small perturbation can just change the parameters. As an example of this, we note the codimension-3 nonlinear stability of the Schwarzschild family by Dafermos–Holzegel–Rodnianski–Taylor [DHRT]. In order to preserve the final black hole parameters, only a codimension-3 submanifold of the moduli space of data is admissible in their theorem.

The stability problem for extremal black holes is exceptional because they suffer from a linear instability known as the *Aretakis instability* [Are11a; Are11b; Are15; Ape22]. This instability is weak, and a restricted form of nonlinear stability is nevertheless conjectured to hold with the same codimensionality as in the subextremal case. See [DHRT, Section IV.2] for conjectures about stability of extremal black holes, [Ang16; AAG20] for stability results on a nonlinear model problem, and numerical work [MRT13; LMRT13] which is consistent with the above conjecture. The Aretakis instability should not be thought of as a manifestation of the third law and understanding its ramifications in the full nonlinear theory is a fundamental open problem in general relativity.

Therefore, asymptotic stability for any fixed parameter ratio (up to and including extremality) should be formulated as a positive codimension statement. In our spherically symmetric setting, we are led to conjecture that for every solution constructed in Corollary 1, there exists a codimension-1 family of perturbations which asymptote to a Reissner–Nordström black hole with the same final parameter ratio. Since the conjectured codimension is the same for every ratio, we are then led to conclude that asymptotically extremal black holes are not qualitatively rarer than any fixed positive temperature.

We hope that our construction demystifies the scenario of matter collapsing to exactly extremal black holes. More generally, the considerations in this paper open up a new window to studying critical behavior in gravitational collapse, which is fundamentally different from the regime studied in [Cho93; GM07].

1.4.6 Aside: Extremal horizons with nearby trapped surfaces

Though not directly relevant for the considerations of the present paper, we would like to point out that there is another issue with the attempt to characterize extremality by the lack of trapped surfaces near the horizon, i.e., by the third property of Definition 1.1. In fact, it would appear that the property of having no trapped surfaces in the interior near the horizon is actually stronger than being extremal.

For a spacetime (\mathcal{M}, g) with Killing field K , a Killing horizon H is said to be *extremal* if the surface gravity κ , defined by $\nabla_K K = \kappa K$ on H , vanishes identically. Equivalently, extremality means that $g(K, K)$ vanishes to at least second order along null geodesics crossing H transversely. If K is timelike to the past of H and $g(K, K)$ vanishes to an *even* order on H , then K passes from timelike, to null, then back to timelike across H , and there are no strictly trapped surfaces near the horizon. This is precisely the situation for extremal Reissner–Nordström and Kerr black holes, where $g(K, K)$ vanishes to second order on the event horizon.

However, there exist spacetimes for which $g(K, K)$ vanishes to an *odd* order (at least three), in which case there may be trapped surfaces just behind the horizon. Indeed, in Proposition A.1 of Appendix A we construct an example of a stationary spacetime containing an extremal Killing horizon, with trapped surfaces just behind the horizon, and satisfying the dominant energy condition. In this case $g(K, K)$ is exactly cubic in an ingoing null coordinate system. It would be interesting to construct such a spacetime with a specific matter model, or an extremal black hole with this behavior.

While extremal Kerr, Reissner–Nordström, and other known examples are extremal in the sense of Definition 1.1, it is far from obvious that all *hair*y (i.e., carrying non-EM matter fields) extremal black holes should be free of trapped surfaces. In view of our example in Appendix A, any mechanism which enforces this must necessarily be global in nature and/or depend on particular properties of the matter model in question.

One could define the notion of a *nondegenerate* extremal Killing horizon, i.e., the Killing field K has the property that $g(K, K)$ vanishes only to second order, which would then be compatible with Definition 1.1. See already Remark A.1.

For more discussion about possible definitions of extremality, see for instance [BF08; Boo16; MRT13].

1.5 Future boundary of the interior and Cauchy horizon gluing

The future boundary of the black hole region of dynamical black holes formed from gravitational collapse in the EMCSF system is known to be intricate (see e.g. [Daf03; Kom13; Van18]). We refer to [Kom13] for a detailed description of the most general possible structure of the interior, but see already Fig. 10 for a summary of the most salient features. In this subsection we will first discuss the future boundary of the black hole interior in Theorem 1. Further, we will present additional corollaries of our characteristic gluing method which provide examples of gravitational collapse to black holes with a piece of null boundary (a “Cauchy horizon”) and a construction of spacetimes for which a Cauchy horizon closes off the interior region.

1.5.1 Future boundary of the interior in Theorem 1

For our main counterexample to the third law in Theorem 1, we obtain that the regular center Γ extends into the black hole region. Regarding the future boundary of the spacetime, we do not know whether there exists a piece of possibly singular null boundary emanating from i^+ as in the subextremal case [Daf03; Van18] or whether a spacelike singularity emanates from i^+ . Note that the result of [GL19], which shows the existence of a Cauchy horizon emanating from i^+ , does not apply directly since their analysis requires $|\mathfrak{c}|M \leq 0.1$, whereas our construction requires $|\mathfrak{c}|M$ large. Nevertheless, one may speculate that a piece of Cauchy horizon occurs (for which the linear analysis of [Gaj17a; Gaj17b] would be relevant), which could eventually turn into a spacelike singularity. (Note that one can readily set up the data such that the future boundary of the interior in Theorem 1 has a piece of spacelike singularity. See however already Section 1.5.3.)

1.5.2 Gravitational collapse with a piece of smooth Cauchy horizon

Another corollary of our method is the construction of regular one-ended Cauchy data which evolve to a subextremal or extremal black hole for which there exists a piece of Cauchy horizon emanating from i^+ . We refer to Fig. 6 for the Penrose diagram of the spacetime constructed in Corollary 2. The proof of Corollary 2 is given in Section 5.4.

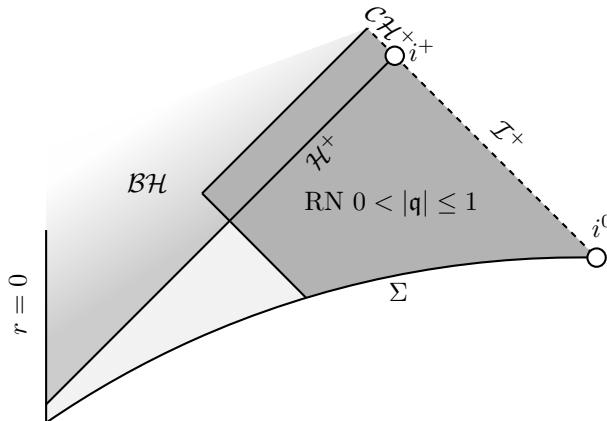


Figure 6: Penrose diagram depicting Corollary 2: Gravitational collapse to Reissner–Nordström with nonempty piece of Cauchy horizon \mathcal{CH}^+ .

Corollary 2 (Gravitational collapse to RN with a smooth Cauchy horizon). *For any regularity index $k \in \mathbb{N}$ and nonzero charge to mass ratio $\mathfrak{q} \in [-1, 1] \setminus \{0\}$, there exist spherically symmetric, asymptotically flat Cauchy data for the Einstein–Maxwell-charged scalar field system in spherical symmetry, with $\Sigma \cong \mathbb{R}^3$ and a regular center, such that the maximal future globally hyperbolic development (\mathcal{M}^4, g) has the following properties:*

- The spacetime satisfies all the conclusions of Corollary 1 with $\mathfrak{q} \neq 0$, including C^k -regularity of all dynamical quantities.
- The black hole region contains an isometrically embedded portion of a Reissner–Nordström Cauchy horizon neighborhood with charge to mass ratio \mathfrak{q} .

Remark 1.10. When $|\mathfrak{q}| = 1$, the spacetime constructed in Corollary 2 does not contain trapped symmetry spheres in the dark shaded region in Fig. 6. By a slight modification of the argument in Proposition B.1 below, this implies no trapped surfaces *intersect* the dark shaded region. In particular, the trapped region (in the sense of [HE73, p. 319]) of the spacetime (if nonempty) avoids a whole double null neighborhood of the event horizon. Nevertheless, the event horizon agrees with the outermost apparent horizon for late advanced times.

1.5.3 Black hole interiors for which the Cauchy horizon closes off spacetime

Our horizon gluing method can also be extended to glue Reissner–Nordström interior spheres to a regular center along an ingoing cone, see already Theorem 2C'. Using this, we construct asymptotically flat Cauchy data for which the future boundary of the black hole region \mathcal{BH} is a Cauchy horizon \mathcal{CH}^+ which closes off spacetime. We refer to Fig. 7 for the Penrose diagram of the spacetime constructed in Corollary 3. The proof of Corollary 3 is given in Section 5.5.

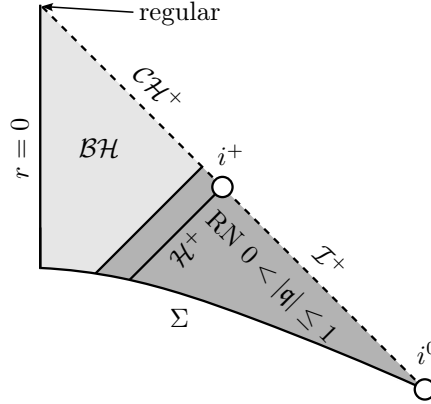


Figure 7: Penrose diagram depicting Corollary 3: The Cauchy horizon is regular and closes off the spacetime in a regular fashion.

Corollary 3 (Cauchy horizon that closes off the spacetime). *For any regularity index $k \in \mathbb{N}$, and nonzero charge to mass ratio $\mathfrak{q} \in [-1, 1] \setminus \{0\}$, there exist spherically symmetric, asymptotically flat Cauchy data for the Einstein–Maxwell-charged scalar field system, with $\Sigma \cong \mathbb{R}^3$ and a regular center, such that the maximal future globally hyperbolic development (\mathcal{M}^4, g) has the following properties:*

- All dynamical quantities are at least C^k -regular.
- The black hole region is non-empty, $\mathcal{BH} \doteq \mathcal{M} \setminus J^-(\mathcal{I}^+) \neq \emptyset$.
- The future boundary of \mathcal{BH} is a C^k -regular Cauchy horizon \mathcal{CH}^+ which closes off spacetime.
- The black hole exterior is isometric to a Reissner–Nordström exterior with charge to mass ratio \mathfrak{q} . In particular, null infinity \mathcal{I}^+ is complete.
- The spacetime does not contain antitrapped surfaces.
- When $|\mathfrak{q}| = 1$, the spacetime does not contain trapped surfaces.

Remark 1.11. In contrast to our previous constructions, the Cauchy surface Σ in Corollary 3 could contain trapped surfaces and Σ intersects the black hole region. It would be interesting to construct a spacetime as in Corollary 3 which depicts genuine gravitational collapse, i.e., for which $\Sigma \subset J^-(\mathcal{I}^+)$.

In the subextremal case, the behavior exhibited by our construction can be seen as exceptional as one generically expects a Cauchy horizon which forms in gravitational collapse to be a weak null singularity [Daf03; Van18; LO19]. In particular, in the case where the Cauchy horizon \mathcal{CH}^+ is weakly singular, Van de Moortel [Van19] showed that the Cauchy horizon \mathcal{CH}^+ cannot close off spacetime in the sense of Fig. 7. Thus, our construction in Corollary 3 makes [Van19] sharp in the sense that the singularity assumption of \mathcal{CH}^+ in [Van19] is needed. Restricted to the extremal case, however, on the basis of a more regular Cauchy horizon as in [GL19], one may speculate that there exists a set of data (open as a subset of the positive codimension set of data settling down to ERN) for which the Cauchy horizon closes off spacetime as depicted in Fig. 7.

Acknowledgments

The authors wish to express their gratitude to Mihalis Dafermos for suggesting the problem and many helpful discussions. We also thank Jonathan Luk, Hamed Masood, Thomas Massoni, Georgios Moschidis, Harvey Reall, Igor Rodnianski, Jaydeep Singh, and Nina Zubrilina for helpful conversations. C.K. acknowledges support by a grant from the Institute for Advanced Study, by Dr. Max Rössler, the Walter Haefner Foundation, and the ETH Zürich Foundation. R.U. acknowledges partial support from the grant NSF-1759835 and the hospitality of the Institute for Advanced Study, the Centro de Ciencias de Benasque, and the University of Cambridge.

2 The characteristic initial value problem for the Einstein–Maxwell-charged scalar field system in spherical symmetry

In this section, we give a detailed explanation of the setup and characteristic initial value problem for the Einstein equations with charged scalar fields in spherical symmetry, with a view towards the characteristic gluing problem. See [Kom13] for more details on the EMCSF system.

2.1 The Einstein–Maxwell-charged scalar field system in spherical symmetry

2.1.1 Spherically symmetric spacetimes

We say that a smooth, connected, time-oriented, four-dimensional Lorentzian manifold (\mathcal{M}, g) is a *spherically symmetric* spacetime with (possibly empty) center of symmetry $\Gamma \subset \mathcal{M}$ if $\mathcal{M} \setminus \Gamma$ splits diffeomorphically as $\mathcal{M} \setminus \Gamma \cong \mathring{\mathcal{Q}} \times S^2$ with metric

$$g = g_{\mathcal{Q}} + r^2 g_{S^2},$$

where $(\mathcal{Q}, g_{\mathcal{Q}})$ for $\mathcal{Q} = \mathring{\mathcal{Q}} \cup \Gamma$ is a (1+1)-dimensional Lorentzian spacetime with (possibly empty) boundary Γ , g_{S^2} is the round metric on the sphere, and $r: \mathcal{Q} \rightarrow \mathbb{R}_{\geq 0}$ is a function which can be geometrically interpreted as the area radius of the orbits of the isometric $\text{SO}(3)$ action on (\mathcal{M}, g) . In mild abuse of notation, we denote with Γ both the center of symmetry in \mathcal{M} and its projection to \mathcal{Q} . Moreover, if Γ is non-empty, we assume that the $\text{SO}(3)$ action fixes Γ and that Γ consists of one timelike geodesic along which $r = 0$. We further assume that $(\mathcal{Q}, g_{\mathcal{Q}})$ admits a global double-null foliation (locally a double-null foliation always exists) with null coordinates (u, v) such that the metric g takes the form

$$g = -\Omega^2 du dv + r^2 g_{S^2}$$

for a nowhere vanishing function $\Omega^2 = -2g_{\mathcal{Q}}(\partial_u, \partial_v)$ on \mathcal{Q} and such that ∂_u and ∂_v are future-directed. We further assume that along the center Γ , the coordinate v is outgoing and u is ingoing, i.e., $\partial_v r|_{\Gamma} > 0$, $\partial_u r|_{\Gamma} < 0$. While we introduced the above notions in the smooth category, we will also consider spacetimes which are less regular ($C^{k \geq 1}$). We note that all notions introduced above also apply in this less regular case. We will also make use of the Hawking mass $m: \mathcal{M} \rightarrow \mathbb{R}$ defined as

$$m \doteq \frac{r}{2}(1 - g(\nabla r, \nabla r))$$

which also can be viewed as a function on \mathcal{Q} as

$$m = \frac{r}{2} \left(1 + 4 \frac{\partial_u r \partial_v r}{\Omega^2} \right). \quad (2.1)$$

Finally, we note that the double null coordinates (u, v) are not unique and for any smooth functions $U, V: \mathbb{R} \rightarrow \mathbb{R}$ with $U', V' > 0$, we obtain new global double null coordinates $(\tilde{u}, \tilde{v}) = (U(u), V(v))$ such that the metric $g = -\tilde{\Omega}^2 d\tilde{u}d\tilde{v} + r^2 g_{S^2}$, where $\tilde{\Omega}^2(\tilde{u}, \tilde{v}) = (U'V')^{-1} \Omega^2(U^{-1}(\tilde{u}), V^{-1}(\tilde{v}))$ and $r(\tilde{u}, \tilde{v}) = r(U^{-1}(\tilde{u}), V^{-1}(\tilde{v}))$.

2.1.2 The Einstein–Maxwell-charged scalar field system

For the Einstein–Maxwell-scalar field system (1.1)–(1.5) in spherical symmetry, additionally to the spherically symmetric spacetime (\mathcal{M}^4, g) , we assume that the field ϕ is complex-valued and spherically symmetric, so that ϕ descends to a function $\mathcal{Q} \rightarrow \mathbb{C}$, and that F and A are spherically symmetric such that F can be written as

$$F = \frac{Q}{2r^2} \Omega^2 du \wedge dv$$

for charge $Q: \mathcal{Q} \rightarrow \mathbb{R}$. The potential 1-form reads

$$A = A_u du + A_v dv.$$

We also define the gauge covariant derivative operator $D = d + i\epsilon A$. The Einstein–Maxwell-scalar field system is invariant with respect to the following gauge transformations

$$\phi \mapsto e^{-i\epsilon\chi} \phi, \quad A \mapsto A + d\chi \quad (2.2)$$

for real-valued functions $\chi = \chi(u, v)$, where ϵ is a dimensionful coupling constant representing the charge of the scalar field. More abstractly, the Einstein–Maxwell-scalar field system is a $U(1)$ -gauge theory and we refer to [Kom13] for more details. In order to break the symmetry we will use the global electromagnetic gauge

$$A_v = 0 \quad (2.3)$$

throughout the paper. In this gauge, the Einstein–Maxwell-scalar field system (1.1)–(1.3) in spherical symmetry reduces to the following set of equations.

Wave equations for scalar field and metric components:

$$\partial_u \partial_v \phi = -\frac{\partial_u \phi \partial_v r}{r} - \frac{\partial_u r \partial_v \phi}{r} + \frac{i\epsilon \Omega^2 Q}{4r^2} \phi - i\epsilon A_u \frac{\partial_v r}{r} \phi - i\epsilon A_u \partial_v \phi \quad (2.4)$$

$$\partial_u \partial_v r = -\frac{\Omega^2}{4r} - \frac{\partial_u r \partial_v r}{r} + \frac{\Omega^2}{4r^3} Q^2 \quad (2.5)$$

$$\partial_u \partial_v \log(\Omega^2) = \frac{\Omega^2}{2r^2} + 2 \frac{\partial_u r \partial_v r}{r^2} - \frac{\Omega^2}{r^4} Q^2 - 2\text{Re}(D_u \phi \overline{\partial_v \phi}) \quad (2.6)$$

Maxwell's equations:

$$\partial_u Q = -\epsilon r^2 \text{Im}(\phi \overline{D_u \phi}) \quad (2.7)$$

$$\partial_v Q = \epsilon r^2 \text{Im}(\phi \overline{\partial_v \phi}) \quad (2.8)$$

$$\partial_v A_u = -\frac{Q \Omega^2}{2r^2} \quad (2.9)$$

Raychaudhuri's equations:

$$\partial_u \left(\frac{\partial_u r}{\Omega^2} \right) = -\frac{r}{\Omega^2} |D_u \phi|^2 \quad (2.10)$$

$$\partial_v \left(\frac{\partial_v r}{\Omega^2} \right) = -\frac{r}{\Omega^2} |\partial_v \phi|^2 \quad (2.11)$$

From these equations we easily derive

$$\partial_v(r\partial_u r) = -\frac{\Omega^2}{4} \left(1 - \frac{Q^2}{r^2}\right) \quad (2.12)$$

and

$$\partial_v\partial_u(r\phi) = -\frac{\Omega^2 m}{2r^2}\phi + i\frac{\epsilon\Omega^2 Q}{4r}\phi + \frac{\Omega^2 Q^2}{4r^3}\phi - i\epsilon A_u\partial_v(r\phi), \quad (2.13)$$

as well as

$$\partial_v m = 2\Omega^{-2}r^2(-\partial_u r)|\partial_v\phi|^2 + \frac{1}{2}\frac{Q^2}{r^2}\partial_v r \quad (2.14)$$

which will be useful later.

2.2 The characteristic initial value problem

With the equations of the EMCSF system at hand, we can precisely define what we mean by a C^k solution. We may for now restrict attention to solutions away from the center.

2.2.1 Bifurcate characteristic data

Definition 2.1. Let $k \in \mathbb{N}$. A C^k solution for the Einstein–Maxwell-charged scalar field system in the EM gauge (2.3) consists of a domain $\mathcal{Q} \subset \mathbb{R}_{u,v}^{1+1}$ and functions $r \in C^{k+1}(\mathcal{Q})$ and $\Omega^2, \phi, Q, A_u \in C^k(\mathcal{Q})$, such that $r > 0$, $\Omega^2 > 0$, ϕ is complex-valued, $\partial_v^{k+1}A_u \in C^0(\mathcal{Q})$, and the functions satisfy equations (2.4)–(2.11).

Next, we formulate the characteristic initial value problem for this class of solutions. Let $\mathbb{R}_{u,v}^{1+1}$ denote the standard $(1+1)$ -dimensional Minkowski space. We introduce the *bifurcate null hypersurface* $C \cup \underline{C} \subset \mathbb{R}_{u,v}^{1+1}$, where

$$\begin{aligned} C &\doteq C_{-1} \doteq \{u = -1\} \cap \{v \geq 0\} \\ \underline{C} &\doteq \underline{C}_0 \doteq \{v = 0\} \cap \{u \geq -1\}. \end{aligned}$$

The special point $(-1, 0)$ is called the *bifurcation sphere*. We pose data for ϕ , Q , r , Ω^2 and A_u for the Einstein–Maxwell-charged-scalar field system on $C \cup \underline{C}$.

Definition 2.2. Let $k \in \mathbb{N}$. A C^k *bifurcate characteristic initial data set* on $C \cup \underline{C}$ for the Einstein–Maxwell-charged scalar field system in the EM gauge (2.3) consists of continuous functions $r > 0$, $\Omega^2 > 0$, ϕ (complex-valued), Q , and A_u on $C \cup \underline{C}$. It is required that $r \in C^{k+1}$, $\Omega^2 \in C^k$, $\phi \in C^k$, $Q \in C^k$, and $A_u \in C^k$ on $C \cup \underline{C}$.³ Finally, the data are required to satisfy equations (2.7)–(2.11), which implies also $\partial_v^{k+1}A_u \in C^0(C)$.

Given characteristic initial data on a portion of $C \cup \underline{C}$ containing the bifurcation sphere, we can solve in a full double null neighborhood to the future. The proof is a standard iteration argument.

Proposition 2.1. *Given a C^k bifurcate characteristic initial data set for the EMCSF system on*

$$(\{u = -1\} \times \{0 \leq v \leq v_0\}) \cup (\{-1 \leq u \leq u_0\} \times \{v = 0\}) \subset C \cup \underline{C},$$

where $u_0 > -1$ and $v_0 > 0$, there exists a number $\delta > 0$ and a unique spherically symmetric C^k solution of the EMCSF system on

$$(\{-1 \leq u \leq -1 + \delta\} \times \{0 \leq v \leq v_0\}) \cup (\{-1 \leq u \leq u_0\} \times \{0 \leq v \leq \delta\})$$

which extends the initial data on $C \cup \underline{C}$.

²Note that the wave equations (2.4) and (2.6) can readily be interpreted for $k = 1$.

³By “ C^k on $C \cup \underline{C}$ ” is meant that v derivatives are continuous on C and u derivatives are continuous on \underline{C} .

2.2.2 Determining transversal derivatives from tangential data

Now that we know that the data on $C \cup \underline{C}$ extends to a solution of the system (2.4)–(2.11), we can use the equations to compute all the partial derivatives of the solution along $C \cup \underline{C}$. We describe a procedure for determining all u -derivatives on C just in terms of r, Ω^2, ϕ, Q , and A_u (as functions of v) and their u derivatives at the bifurcation sphere.

Proposition 2.2. *Let $(r, \Omega^2, \phi, Q, A_u)$ be a C^k bifurcate characteristic initial data set as in Definition 2.2. Then the EMCSF system can be used to determine as many u -derivatives of r, Ω^2, ϕ, Q , and A_u on C as is consistent with Definition 2.1, explicitly from the data on $C \cup \underline{C}$.*

Proof. Since $(r, \Omega^2, \phi, Q, A_u)$ are all given on \underline{C} , we can compute as many u -derivatives of these quantities at the bifurcation sphere $(-1, 0)$ as the regularity k allows. We describe an inductive procedure for computing u -derivatives of $(r, \Omega^2, \phi, Q, A_u)$ on C , starting with $\partial_u r$. Since $\partial_u r(-1, 0)$ is known, and the wave equation (2.5) can be written as

$$\left(\partial_v + \frac{\partial_v r}{r} \right) \partial_u r = -\frac{\Omega^2}{4r} + \frac{\Omega^2}{4r^3} Q^2,$$

where everything on the right-hand side is already known, $\partial_u r(-1, v)$ can be found by solving this ODE. In the same manner, $\partial_u \phi(-1, v)$ and then $\partial_u \log(\Omega^2)(-1, v)$ can be found. To find $\partial_u Q(-1, v)$, differentiate (2.7) in v and then integrate. (Alternatively, differentiate (2.8) in u .) Finally, $\partial_u A_u(-1, v)$ is found by differentiating (2.9) in v and then integrating.

Proceeding in this way, by commuting all the equations with ∂_u^i , every partial derivative of $(r, \Omega^2, \phi, Q, A_u)$ which is consistent with the initial C^k regularity can be found. We finally note that $\partial_u^{k+1} r(-1, v)$ is found from differentiating (2.10) an appropriate number of times, since the wave equation it satisfies is not consistent with the level of regularity of the rest of the dynamical variables. \square

Remark 2.1. Both Proposition 2.1 and Proposition 2.2 exploit the *null condition* satisfied by the EMCSF system in double null gauge. For a general nonlinear wave equation, the solution may not exist in a full double null neighborhood of the initial bifurcate null hypersurface as in Proposition 2.1. Indeed, the null condition means the transport equations for transversal derivatives in Proposition 2.2 are linear and hence do not blow up in finite time.

2.3 Sphere data and cone data

2.3.1 Sphere data

In order to define a notion of characteristic gluing later, we introduce a notion of *sphere data* inspired by [ACR21a; ACR21b]. Given a C^k solution of the EMCSF system in spherical symmetry, for every $(u_0, v_0) \in \mathcal{Q}$ one can extract a list of numbers corresponding to $r(u_0, v_0)$, $\Omega^2(u_0, v_0)$, $\phi(u_0, v_0)$, $Q(u_0, v_0)$, $\partial_u r(u_0, v_0)$ etc. Our definition of sphere data formalizes this (long) list of numbers and incorporates the constraints (2.7)–(2.11), so we may refer to the data induced by a C^k solution on a sphere without reference to an actual solution of the equations themselves.

Definition 2.3. Let $k \geq 1$. A *sphere data set* with *regularity index* k for the Einstein–Maxwell-charged scalar field in the EM gauge (2.3) is the following list of numbers⁴:

1. $\varrho > 0, \varrho_u^1, \dots, \varrho_u^{k+1}, \varrho_v^1, \dots, \varrho_v^{k+1} \in \mathbb{R}$
2. $\omega > 0, \omega_u^1, \dots, \omega_u^k, \omega_v^1, \dots, \omega_v^k \in \mathbb{R}$
3. $\varphi, \varphi_u^1, \dots, \varphi_u^k, \varphi_v^1, \dots, \varphi_v^k \in \mathbb{C}$
4. $q, q_u^1, \dots, q_u^k, q_v^1, \dots, q_v^k \in \mathbb{R}$
5. $a, a_u^1, \dots, a_u^k, a_v^1, \dots, a_v^k, a_v^{k+1} \in \mathbb{R}$

subject to the following conditions:

⁴One should think that formally $r(u_0, v_0) = \varrho$, $\phi(u_0, v_0) = \varphi$, $\Omega^2(u_0, v_0) = \omega$, $\partial_v^i r(u_0, v_0) = \varrho_v^i$, etc.

- (i) ϱ_u^{i+2} can be expressed as a rational function of ϱ_u^{j+1} , ω_u^{j+1} , φ_u^{j+1} , and a_u^j for $0 \leq j \leq i$ by formally differentiating (2.10),
- (ii) ϱ_v^{i+2} can be expressed as a rational function of ϱ_v^{j+1} , ω_v^{j+1} , and φ_v^{j+1} for $0 \leq j \leq i$ by formally differentiating (2.11),
- (iii) q_u^{i+1} can be expressed as a polynomial of ϱ_u^j , φ_u^j , and a_u^j for $0 \leq j \leq i$ by formally differentiating (2.7),
- (iv) q_v^{i+1} can be expressed as a polynomial of ϱ_v^j , and φ_v^j for $0 \leq j \leq i$ by formally differentiating (2.8), and
- (v) a_v^{i+1} can be expressed as a rational function of ϱ_v^j , ω_v^j , and q_v^j for $0 \leq j \leq i$ by formally differentiating (2.9),

where we have adopted the convention that $\varrho_u^0 = \varrho$, etc. We denote by \mathcal{D}_k the set of such sphere data sets with regularity index k .

Gauge freedom is a very important aspect of the study of the EMCSF system. Our next definition records the gauge freedom present in sphere data. We need to consider both double null gauge transformations

$$u = f(U), \quad v = g(V),$$

where f and g are increasing functions on \mathbb{R} and EM gauge transformations (2.2)

$$\phi \mapsto e^{-i\epsilon\chi}\phi, \quad A \mapsto A + d\chi,$$

where χ is a function of u alone, i.e. $\partial_v\chi = 0$, in order to satisfy (2.3).

Definition 2.4. We define the *full gauge group* of the Einstein–Maxwell-charged scalar field system in spherically symmetric double null gauge with the EM gauge condition (2.3) as

$$\mathcal{G} \doteq \{(f, g) : f, g \in \text{Diff}_+(\mathbb{R}), f(0) = g(0) = 0\} \times C^\infty(\mathbb{R}),$$

with the group multiplication given by⁵

$$((f_2, g_2), \chi_2) \cdot ((f_1, g_1), \chi_1) = ((f_2 \circ f_1, g_2 \circ g_1), \chi_2 \circ f_1^{-1} + \chi_1).$$

The gauge group defines an action on sphere data as follows. Given sphere data $D \in \mathcal{D}_k$, assign functions $r(u, v)$, $\Omega^2(u, v)$, $\phi(u, v)$, $Q(u, v)$, and $A_u(u, v)$ whose jets agree with the sphere data D . For $\tau = ((f, g), \chi) \in \mathcal{G}$, let

$$\tilde{r}(u, v) = r(f(u), g(v)) \tag{2.15}$$

$$\tilde{\Omega}^2(u, v) = f'(u)g'(v)\Omega^2(f(u), g(v)) \tag{2.16}$$

$$\tilde{\phi}(u, v) = e^{-i\epsilon\chi(f(u))}\phi(f(u), g(v)) \tag{2.17}$$

$$\tilde{Q}(u, v) = Q(f(u), g(v)) \tag{2.18}$$

$$\tilde{A}_u(u, v) = f'(u)A_u(f(u)) + f'(u)\chi'(f(u)). \tag{2.19}$$

The components of τD are then defined by formally differentiating equations (2.15)–(2.19) and evaluating at $u = v = 0$. For example, $\tau(\varrho) = \varrho$, $\tau(\varrho_v^1) = g'(0)\varrho_v^1$, and $\tau(\varphi_u^1) = (1 - i\epsilon\chi'(0))e^{-i\epsilon\chi(0)}\varphi$.

If one is given a bifurcate characteristic initial data set $(r, \Omega^2, \phi, Q, A_u)$, the lapse Ω^2 can be set to unity on $C \cup \underline{C}$ by reparametrizing u and v . In the sphere data setting, we have an analogous notion:

Definition 2.5. A sphere data set $D \in \mathcal{D}_k$ is said to be *lapse normalized* if $\omega = 1$ and $\omega_u^i = \omega_v^i = 0$ for $1 \leq i \leq k$. Every sphere data set is gauge equivalent to a lapse normalized sphere data set.

⁵One can view this as a left semidirect product.

2.3.2 Cone data and seed data

In the previous subsection, we saw how a C^k solution $(r, \Omega^2, \phi, Q, A_u)$ on \mathcal{Q} gives rise to a continuous map $\mathcal{Q} \rightarrow \mathcal{D}_k$. For the purpose of characteristic gluing, it is convenient to consider one-parameter families of sphere data which are to be thought of as being induced by constant u cones in \mathcal{Q} .

More precisely, if we consider a null cone $C \subset \mathcal{Q}$, parametrized by $v \in [v_1, v_2]$, then a solution of the EMCSF system induces a continuous map $D : [v_1, v_2] \rightarrow \mathcal{D}_k$ by sending each v to its associated sphere data $D(v)$. In fact, this map can be produced by knowing only $D(v_1)$ and the values of $(r, \Omega^2, \phi, Q, A_u)$ on C . Arguing as in Proposition 2.2 with $D(v_1)$ taking the role of the bifurcation sphere gives:

Proposition 2.3. *Let $k \in \mathbb{N}$, $v_1 < v_2 \in \mathbb{R}$, $r, A_u \in C^{k+1}([v_1, v_2])$, and $\Omega^2, \phi, Q \in C^k([v_1, v_2])$ which satisfy the constraints (2.8), (2.9), and (2.11) on $[v_1, v_2]$. Let $D_1 \in \mathcal{D}_k$ such that all v -components of D_1 agree with the corresponding v -derivatives of $(r, \Omega^2, \phi, Q, A_u)$ at v_1 . Then there exists a unique continuous function $D : [v_1, v_2] \rightarrow \mathcal{D}_k$ such that $D(v_1) = D_1$ and upon identification of the formal symbols $\varrho(D(v))$, $\varrho_u^1(D(v))$, etc., with the dynamical variables $(r, \Omega^2, \phi, Q, A_u)$ and their u - and v -derivatives, satisfies the EMCSF system and agrees with $(r, \Omega^2, \phi, Q, A_u)$ in the v -components for every $v \in [v_1, v_2]$.*

Definition 2.6. Let $k \in \mathbb{N}$ and $v_1 < v_2 \in \mathbb{R}$. A C^k cone data set for the Einstein–Maxwell-charged scalar field in spherical symmetry is a continuous function $D : [v_1, v_2] \rightarrow \mathcal{D}_k$ satisfying the conclusion of Proposition 2.3, i.e., formally satisfying the EMCSF system.

We now discuss a procedure for generating solutions of the “tangential” constraint equations, (2.8), (2.9), and (2.11), which were required to be satisfied in the previous proposition.

Proposition 2.4 (Seed data). *Let $k \in \mathbb{N}$, $v_1 < v_2 \in \mathbb{R}$, and $D_1 \in \mathcal{D}_k$ be lapse normalized. For any $\phi \in C^k([v_1, v_2])$ such that $\partial_v^i \phi(v_1) = \varphi_v^i(D_1)$ for $0 \leq i \leq k$, there exist unique functions $r, A_u \in C^{k+1}([v_1, v_2])$ and $Q \in C^k([v_1, v_2])$ such that $(r, \Omega^2, \phi, Q, A_u)$ satisfies the hypotheses of Proposition 2.3 with $\Omega^2(v) = 1$ for every $v \in [v_1, v_2]$.*

Proof. When $\Omega^2 \equiv 1$, Raychaudhuri’s equation (2.11) reduces to

$$\partial_v^2 r = -r |\partial_v \phi|^2,$$

which is a second order ODE for $r(v)$. Setting $r(v_1) = \varrho(D_1)$ and $\partial_v r(v_1) = \varrho_v^1(D_1)$, we obtain a unique solution $r \in C^{k+1}([v_1, v_2])$. The charge is obtained by integrating Maxwell’s equation (2.8):

$$Q(v) = q(D_1) + \int_0^v \epsilon r^2(v') \operatorname{Im}(\phi(v') \overline{\partial_v \phi(v')}) dv'.$$

Finally, the gauge potential is obtained by integrating (2.9):

$$A_u(v) = a(D_1) - \int_0^v \frac{Q(v')}{2r^2(v')} dv'.$$

The v -derivatives of $(r, \Omega^2, \phi, Q, A_u)$ agree with the v -components of D_1 by virtue of the definitions. \square

3 The main gluing theorems

In this section we give precise statements of our main theorems. In order to do this, we carefully define the notion of *characteristic gluing*.

3.1 Characteristic gluing in spherical symmetry

Definition 3.1 (Characteristic gluing). Let $k \in \mathbb{N}$. Let $D_1, D_2 \in \mathcal{D}_k$ be sphere data sets. We say that D_1 can be *characteristically glued to D_2 to order k* in the Einstein–Maxwell-charged scalar field system in spherical symmetry if there exist $v_1 < v_2$ and a C^k cone data set $D : [v_1, v_2] \rightarrow \mathcal{D}_k$ such that $D(v_1)$ is gauge equivalent to D_1 and $D(v_2)$ is gauge equivalent to D_2 .

Remark 3.1. It is clear that if D_1 and D_2 can be characteristically glued and $\tau_1, \tau_2 \in \mathcal{G}$, then $\tau_1 D_1$ and $\tau_2 D_2$ can be characteristically glued.

Remark 3.2. Definition 3.1 on characteristic gluing along an outgoing cone has a natural analog defining characteristic gluing along an ingoing cone by parametrizing the cone data with u and letting v denote the transverse null coordinate, but keeping the definition of sphere data unchanged.

By Proposition 2.4, characteristic gluing is equivalent to choosing an appropriate seed ϕ in the following sense. By applying a gauge transformation to D_1 , we may assume it to be lapse normalized. Then cone data sets with $\Omega^2 \equiv 1$ agreeing with D_1 at v_1 are parametrized precisely by functions $\phi \in C^k([v_1, v_2]; \mathbb{C})$ with the correct v -jet at v_1 . Therefore, characteristic gluing reduces to finding ϕ so that the final data set $D(v_2)$ produced by Proposition 2.3 is gauge equivalent to D_2 .

3.2 Spacetime gluing from characteristic gluing

If the two sphere data sets in Definition 3.1 come from spheres in two spherically symmetric EMCSF spacetimes, we can use local well posedness for the EMCSF characteristic initial value problem, Proposition 2.1, to glue parts of the spacetimes themselves. This principle underlies all of our constructions in Section 5.

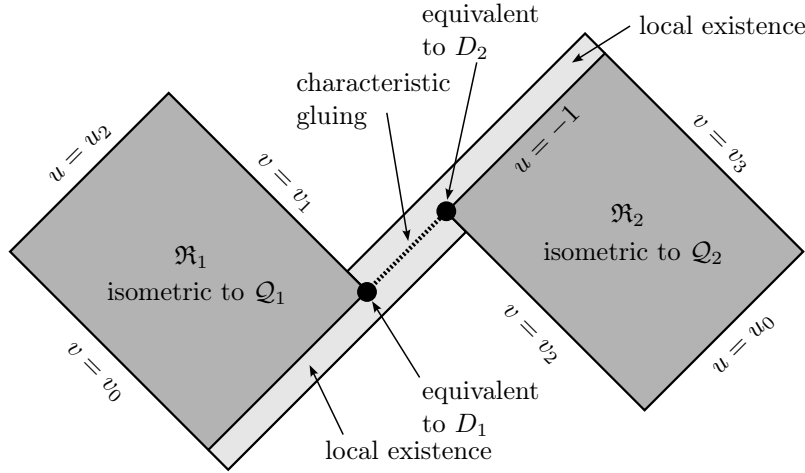


Figure 8: Spacetime gluing obtained from characteristic gluing. The two spacetimes (dark gray) are glued along the cone $u = -1$. Note that the dark gray regions are causally disconnected except for the cone $u = -1$. Such a spacetime exists if and only if D_1 and D_2 can be characteristically glued.

Proposition 3.1. *Let $(\mathcal{Q}_1, r_1, \Omega_1^2, \phi_1, Q_1, A_{u1})$ and $(\mathcal{Q}_2, r_2, \Omega_2^2, \phi_2, Q_2, A_{u2})$ be two C^k solutions of the EMCSF system in spherical symmetry, where each \mathcal{Q}_i is a double null rectangle, i.e.,*

$$\begin{aligned} \mathcal{Q}_1 &= [u_{0,1}, u_{1,1}] \times [v_{0,1}, v_{1,1}] \\ \mathcal{Q}_2 &= [u_{0,2}, u_{1,2}] \times [v_{0,2}, v_{1,2}]. \end{aligned}$$

Let D_1 be the sphere data induced by the first solution on $(u_{0,1}, v_{1,1})$ and D_2 be the sphere data induced by the second solution on $(u_{1,2}, v_{0,2})$. If D_1 can be characteristically glued to D_2 to order k , then there exists a spherically symmetric C^k solution $(\mathcal{Q}, r, \Omega^2, \phi, Q, A_u)$ of the EMCSF system with the following property: There exists a global double null gauge (u, v) on \mathcal{Q} containing double null rectangles

$$\begin{aligned} \mathfrak{R}_1 &= [-1, u_2] \times [v_0, v_1], \\ \mathfrak{R}_2 &= [u_0, -1] \times [v_2, v_3], \end{aligned}$$

such that the restricted solutions $(\mathfrak{R}_i, r, \Omega^2, \phi, Q, A_u)$ are isometric to the solutions $(\mathcal{Q}_i, r_i, \Omega_i^2, \phi_i, Q_i, A_{u_i})$ for $i = 1, 2$, the sphere data induced on $(-1, v_1)$ is equal to D_1 to k -th order, and the sphere data induced on $(-1, v_2)$ is gauge equivalent to D_2 to k -th order.

Proof. In this proof, we will refer to spherically symmetric solutions of the EMCSF system by their domains alone.

By Definition 3.1, since D_1 and D_2 can be characteristically glued, we obtain $v_1 < v_2$, functions r, Ω^2, ϕ, Q , and A_u on $[v_1, v_2]$, and a gauge transformation $\tau \in \mathcal{D}_k$ which acts on D_2 . We now build the spacetime out of two pieces which will then be pasted along $u = -1$ and match to order C^k . See Fig. 9.

First, we prepare the given spacetimes. We relabel the double null gauge on \mathcal{Q}_1 by changing the southeast edge to be $u = -1$ and the northeast edge to be $v = v_1$. This also determines u_2 and v_0 and we apply no further gauge transformation to \mathcal{Q}_1 . We denote this region by \mathfrak{R}_1 .

Next, the gauge transformation τ is extended and applied to \mathcal{Q}_2 . We relabel the double null gauge to have $u = -1$ on the northwest edge and $v = v_2$ on the southwest edge. We denote this region by \mathfrak{R}_2 .

We now construct the left half of Fig. 9 as follows. Extend the cone $u = -1$ in \mathfrak{R}_1 until $v = v_3$, and extend the functions $(r, \Omega^2, \phi, Q, A_u)$ on $u = -1$ by taking them from the definition of characteristic gluing for $v \in [v_1, v_2]$, and then from the induced data on $u = -1$ in \mathfrak{R}_2 for $v \in [v_2, v_3]$. We now appeal to local existence, Proposition 2.1, the EMCSF system in spherical symmetry to construct the solution in a thin slab \mathcal{S}_1 to the future of

$$(\{u = -1\} \times [v_1, v_3]) \cup ([-1, u_2] \times \{v = v_1\}).$$

This completes the construction of $\mathfrak{R}_1 \cup \mathcal{S}_1$.

The region $\mathfrak{R}_2 \cup \mathcal{S}_2$ is constructed similarly, with the cone $u = -1$ now being extended backwards, first using the characteristic gluing data and then using the tangential data induced by \mathfrak{R}_1 on $u = -1$. Again, Proposition 2.1 is used to construct the thin strip \mathcal{S}_2 .

Finally, the spacetime is constructed by taking $\mathcal{Q} \doteq (\mathfrak{R}_1 \cup \mathcal{S}_1) \cup (\mathfrak{R}_2 \cup \mathcal{S}_2)$ and pasting r, Ω^2, ϕ, Q , and A_u . From the construction, it is clear that the dynamical variables, together with all v -derivatives consistent with C^k regularity are continuous on \mathcal{Q} . To show that all u -derivatives are continuous across $u = -1$, we observe that all transverse quantities are initialized consistently to k -th order at $(-1, v_1)$ and that the tangential data agrees by construction. Now Proposition 2.2 implies that the transverse derivatives through order k are equal on $u = -1$ in both $\mathfrak{R}_1 \cup \mathcal{S}_1$ and $\mathfrak{R}_2 \cup \mathcal{S}_2$. This completes the proof. \square

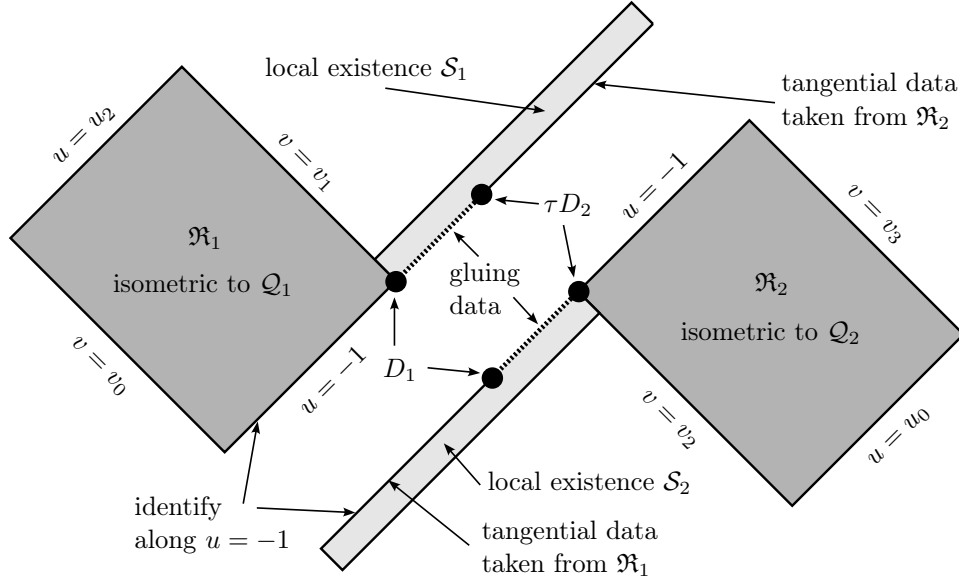


Figure 9: Proof of Proposition 3.1.

Remark 3.3. If the characteristic gluing hypothesis is C^k but no better and the original solutions \mathcal{Q}_1 and \mathcal{Q}_2 are more regular than C^k , then one expects $(k+1)$ -th derivatives of dynamical quantities to jump across any of the null hypersurfaces bordering the light gray regions in Fig. 8.

3.3 Sphere data in Minkowski, Schwarzschild, and Reissner–Nordström

Before stating our main gluing results, we need to precisely define the terms *Minkowski sphere*, *Schwarzschild event horizon sphere*, and *Reissner–Nordström event horizon sphere*.

Definition 3.2 (Minkowski sphere data). Let $k \in \mathbb{N}$ and $R > 0$. The unique lapse normalized sphere data set satisfying

- $\varrho = R$,
- $\varrho_u^1 = -\frac{1}{2}$,
- $\varrho_v^1 = \frac{1}{2}$, and
- all other components zero,

is called the *Minkowski sphere data of radius R* and is denoted by $D_{R,k}^M$.

Definition 3.3 (Schwarzschild sphere data). Let $k \in \mathbb{N}$, $R > 0$, and $0 \leq 2M \leq R$. The unique lapse normalized sphere data set satisfying

- $\varrho = R$,
- $\varrho_u^1 = -\frac{1}{2}$
- $\varrho_v^1 = \frac{1}{2}(1 - 2M/R)$, and
- all other components zero,

is called the *Schwarzschild sphere data of mass M and radius R* and is denoted by $D_{M,R,k}^S$. Note that $D_{0,R,k}^S = D_{R,k}^M$.

Definition 3.4 (Reissner–Nordström horizon sphere data). Let $k \in \mathbb{N}$, $M > 0$, and $0 \leq |e| \leq M$. The unique lapse normalized sphere data set satisfying

- $\varrho = r_+ \doteq M + \sqrt{M^2 - e^2}$,
- $\varrho_u^1 = -\frac{1}{2}$,
- $\varrho_v^1 = 0$,
- $q = e$, and
- all other components zero,

is called the *Reissner–Nordström horizon sphere data with parameters M and e* and is denoted by $D_{M,e,k}^{\text{RNH}}$. Note that $D_{M,0,k}^{\text{RNH}} = D_{M,2M,k}^S$.

We will also define sphere data for general Reissner–Nordström spheres. To do so, we extend the Hawking mass (2.1) to a function on sphere data sets $D \in \mathcal{D}_k$ by setting

$$m(D) \doteq \frac{\varrho}{2} \left(1 + \frac{4\varrho_u^1 \varrho_v^1}{\omega} \right).$$

We also define the *modified Hawking mass* of a spherically symmetric spacetime with charge by

$$\varpi \doteq m + \frac{Q^2}{2r}$$

and extend it to sphere data sets by

$$\varpi(D) \doteq m(D) + \frac{q^2}{2\varrho}.$$

In a Reissner–Nordström spacetime of mass M and charge e , any sphere data set D associated to a symmetry sphere has $\varpi(D) = M$. Note that given $\varrho > 0$, $\varrho_u^1 < 0$, ω , and q , ϱ_v^1 is determined uniquely by $\varpi(D)$.

Recall that the horizons of Reissner–Nordström with parameters $|e| \leq M$ are located at

$$r_{\pm} = M \pm \sqrt{M^2 - e^2}.$$

Definition 3.5 (Reissner–Nordström sphere data). Let $k \in \mathbb{N}$, $e \in \mathbb{R}$, and $R > 0$ satisfy $M > e^2/(2R)$. A lapse normalized sphere data set satisfying

- $\varrho = R$,
- $q = e$,
- $\varpi = M$,
- $|\varrho_v^1| = \frac{1}{2}$, or $|\varrho_u^1| = \frac{1}{2}$, or $\varrho_v^1 = \varrho_u^1 = 0$,
- all other components zero

is called a *Reissner–Nordström sphere data set of modified Hawking mass M , charge e , and radius R* and is denoted by $D_{M,e,R,k}^{\text{RN}}$.

Remark 3.4. A Reissner–Nordström sphere data set of modified Hawking mass M , charge e , and radius R , $D_{M,e,R,k}^{\text{RN}}$, gives rise to unique sphere data if either $\varrho_v^1 = \varrho_u^1 = 0$, or one additionally specifies $\text{sgn}(\varrho_v^1) \in \{+, -\}$ or $\text{sgn}(\varrho_u^1) \in \{+, -\}$.

3.4 Main gluing theorems

With the previous definitions of Section 3.1 and Section 3.3 at hand, we are now in a position to state our main gluing results.

Our first gluing theorem concerns gluing a sphere in Minkowski space to a Schwarzschild event horizon with a *real* scalar field. When the scalar field ϕ in the EMCSF system is real-valued, Maxwell’s equation decouples from the rest of the system and the charge Q is constant throughout the spacetime. Since Q must vanish on any sphere in Minkowski space, it vanishes everywhere and the EMCSF system reduces to the Einstein-scalar field system.

Theorem 2A. *For any $k \in \mathbb{N}$ and $0 < R_i < 2M_f$, the Minkowski sphere of radius R_i , $D_{R_i,k}^{\text{M}}$, can be characteristically glued to the Schwarzschild event horizon sphere with mass M_f , $D_{M_f,k}^{\text{S}}$, to order C^k within the Einstein-scalar field model in spherical symmetry.*

The proof of Theorem 2A is given in Section 4.1. We have separated out Minkowski to Schwarzschild gluing as a special case because it is simpler and highlights our topological argument. We will actually use this special case as the first step to produce our counterexample to the third law in Section 5.3.

Our second gluing theorem concerns gluing a sphere in the domain of outer communication of a Schwarzschild spacetime to a Reissner–Nordström event horizon with specified mass and charge to mass ratio.

Theorem 2B. *For any $k \in \mathbb{N}$, $\mathfrak{q} \in [-1, 1]$, and $\mathfrak{e} \in \mathbb{R} \setminus \{0\}$, there exists a number $M_0(k, \mathfrak{q}, \mathfrak{e}) \geq 0$ such that if $M_f > M_0$, $0 \leq M_i \leq \frac{1}{8}M_f$, and $2M_i < R_i \leq \frac{1}{2}M_f$, then the Schwarzschild sphere of mass M_i and radius R_i , $D_{M_i,R_i,k}^{\text{S}}$, can be characteristically glued to the Reissner–Nordström event horizon with mass M_f and charge to mass ratio \mathfrak{q} , $D_{M_f,\mathfrak{q}M_f,k}^{\text{RNH}}$, to order C^k within the Einstein–Maxwell-charged scalar field model with coupling constant \mathfrak{e} . The associated characteristic data can be chosen to have no spherically symmetric antitrapped surfaces, i.e. $\partial_u r < 0$ everywhere.*

The proof of Theorem 2B is given in Section 4.2.

Remark 3.5. The data constructed in the proof of Theorem 2A will automatically not contain spherically symmetric antitrapped surfaces because of a special monotonicity property in the absence of charge. Namely,

$$\partial_v(r\partial_u r) = -\frac{\Omega^2}{4}, \quad (3.1)$$

so $r\partial_u r$ is decreasing. In particular, since $r\partial_u r$ is negative in Minkowski space, the sign will propagate in view of (3.1) for the Einstein-scalar field model.

Our next gluing theorem supersedes Theorem 2A and Theorem 2B by relaxing the requirement that the final sphere lie on the event horizon. The proof is slightly more involved than Theorem 2B but has the same basic structure and is given in Section 4.3 below.

Theorem 2C. *For any $k \in \mathbb{N}$, $\mathfrak{q} \in \mathbb{R}$, $\mathfrak{e} \in \mathbb{R} \setminus \{0\}$ and $\mathfrak{r} > 0$, there exists a number $M_0(k, \mathfrak{q}, \mathfrak{e}, \mathfrak{r}) > 0$ such that if $M_f > M_0$ and*

$$R_f \geq \frac{M_f}{2}(1 + \mathfrak{r})\mathfrak{q}^2, \quad (3.2)$$

then there exists $R_i \in (0, R_f)$ such that the Minkowski sphere of radius R_i , $D_{R_i, k}^M$, can be characteristically glued to the Reissner–Nordström sphere with modified Hawking mass M_f , charge $\mathfrak{q}M_f$, and radius R_f , $D_{M_f, \mathfrak{q}M_f, R_f, k}^{\text{RN}}$ with $\varrho_u^1 < 0$, to order C^k within the Einstein–Maxwell-charged scalar field system with coupling constant \mathfrak{e} . The associated characteristic data can be chosen to have no spherically symmetric antitrapped surfaces, i.e., $\partial_u r < 0$ everywhere.

Remark 3.6. Reissner–Nordström spheres with modified Hawking mass M , charge $\mathfrak{q}M$ and radius $R \leq \frac{M}{2}\mathfrak{q}^2$ have non-positive Hawking mass, $m \leq 0$. In this sense, the assumption $\mathfrak{r} > 0$ in Theorem 2C is necessary. Indeed, one immediately sees that (3.2) implies

$$m \geq \frac{\mathfrak{r}}{1 + \mathfrak{r}}M_f,$$

so that $\mathfrak{r} > 0$ ensures $m > 0$.

Remark 3.7. Theorem 2C also allows for gluing of Minkowski space to Reissner–Nordström Cauchy horizons located at $r = r_-$. This is achieved by setting $\mathfrak{r} = \mathfrak{q}^2/4$ in Theorem 2C, see already the proof of Corollary 3.

While all the above theorems are stated as gluing results along outgoing cones, by mapping $u \mapsto -v$ and $v \mapsto -u$, they also hold true for gluing along ingoing cones, recall Remark 3.2. In particular, restating Theorem 2C for gluing along ingoing cones gives

Theorem 2C'. *For any $k \in \mathbb{N}$, $\mathfrak{q} \in \mathbb{R}$, $\mathfrak{e} \in \mathbb{R} \setminus \{0\}$ and $\mathfrak{r} > 0$, there exists a number $M_0(k, \mathfrak{q}, \mathfrak{e}, \mathfrak{r}) > 0$ such that if $M_f > M_0$ and*

$$R_f \geq \frac{M_f}{2}(1 + \mathfrak{r})\mathfrak{q}^2, \quad (3.3)$$

then there exists $R_i \in (0, R_f)$ such that the Reissner–Nordström sphere with modified Hawking mass M_f , charge $\mathfrak{q}M_f$, and radius R_f , $D_{M_f, \mathfrak{q}M_f, R_f, k}^{\text{RN}}$ with $\varrho_v^1 > 0$, can be characteristically glued along an ingoing cone to the Minkowski sphere of radius R_i , $D_{R_i, k}^M$, to order C^k within the Einstein–Maxwell-charged scalar field system with coupling constant \mathfrak{e} . The associated characteristic data can be chosen to have no spherically symmetric trapped surfaces, i.e., $\partial_v r > 0$ everywhere.

4 Proofs of the main gluing theorems

We begin with two lemmas which identify the orbits of Schwarzschild and Reissner–Nordström sphere data under the action of the full gauge group. This essentially amounts to a version of Birkhoff’s theorem for sphere data.

Lemma 4.1 (Schwarzschild exterior sphere identification). *If $D \in \mathcal{D}_k$ satisfies*

- $\varrho = R > 0$,
- $\varrho_u^1 < 0$,
- $\varrho_v^1 > 0$,
- $\frac{1}{2}\varrho(1 + 4\varrho_u^1\varrho_v^1) = M$,
- $q = 0$, and
- $\varphi_u^i = \varphi_v^i = 0$ for $0 \leq i \leq k$,

then $R > 2M$ and D is equivalent to $D_{M, R, k}^S$ up to a gauge transformation.

Proof. First, we observe that by the relations obtained from Maxwell's equations, $q_u^i = q_v^i = 0$ for $1 \leq i \leq k$. Since $\varphi_u^i = \varphi_v^i = 0$, we can perform an EM gauge transformation to make $a_u^i = 0$ for $0 \leq i \leq k$. Also, $a_v^i = 0$ for $1 \leq i \leq k$ from $F = d(A_u du)$. Next, we can normalize the lapse. Finally, $R > 2M$ follows from the definitions and $\varrho_u^1 \varrho_v^1 < 0$. \square

Lemma 4.2 (Reissner–Nordström horizon sphere identification). *If $D \in \mathcal{D}_k$ satisfies*

- $\varrho = (1 + \sqrt{1 - \mathfrak{q}^2})M$ for $\mathfrak{q} \in [-1, 1]$ and $M > 0$,
- $\varrho_u^1 < 0$,
- $\varrho_v^1 = 0$,
- $q = \mathfrak{q}M$, and
- $\varphi_u^i = \varphi_v^i = 0$ for $0 \leq i \leq k$,

then D is equivalent to $D_{M, \mathfrak{q}M, k}^{\text{RN}}$ up to a gauge transformation.

Proof. As before, the charge vanishes to all orders and we normalize the gauge potential and lapse. We then use the additional double null gauge freedom $u \mapsto \lambda u$, $v \mapsto \lambda^{-1}v$ to make $\varrho_u^1 = -\frac{1}{2}$. \square

Remark 4.1. Without the condition $\varrho_u^1 < 0$ in the previous lemma, the sphere data in the extremal case could also arise from the *Bertotti–Robinson* universe.

With these lemmas and Remark 3.1 in mind, we follow the strategy discussed in Section 3.1. We fix the interval $[0, 1]$, set $\Omega^2 \equiv 1$, and solve Raychaudhuri's equation, Maxwell's equation, and the transport equation for transverse derivatives of ϕ with appropriate initial and final values. We do **not** have to track transverse derivatives of $\partial_u r$, Ω^2 , Q , or A_u , because these will be “gauged away” at the end of the proof.

4.1 Proof of Theorem 2A

In this subsection we prove Theorem 2A. We first note that if the scalar field is chosen to be real-valued, the Einstein–Maxwell-charged scalar field system collapses to the Einstein-scalar field system. If the initial data has no charge ($Q(0) = 0$), then this is equivalent to setting $\mathfrak{e} = 0$ and A_u and all its derivatives to be identically zero.

We will first set up our scalar field ansatz as a collection of pulses. To do so, let

$$0 = v_0 < v_1 < \cdots < v_k < v_{k+1} = 1$$

be an arbitrary partition of $[0, 1]$. For each $1 \leq j \leq k+1$, fix a nontrivial bump function

$$\chi_j \in C_c^\infty((v_{j-1}, v_j); \mathbb{R}).$$

In the rest of this section, the functions $\chi_1, \dots, \chi_{k+1}$ are fixed and our constructions depend on these choices.

Let $\alpha = (\alpha_1, \dots, \alpha_{k+1}) \in \mathbb{R}^{k+1}$ and set

$$\phi_\alpha(v) \doteq \phi(v; \alpha) \doteq \sum_{1 \leq j \leq k+1} \alpha_j \chi_j(v). \quad (4.1)$$

We set $\Omega^2(v; \alpha) \equiv 1$ along $[0, 1]$ and define $r(v; \alpha)$ as the unique solution of Raychaudhuri's equation (2.11) with this scalar field ansatz,

$$\partial_v^2 r(v; \alpha) = -r(v; \alpha) (\partial_v \phi_\alpha(v))^2, \quad (4.2)$$

with prescribed “final values”

$$\begin{aligned} r(1; \alpha) &= 2M_f \\ \partial_v r(1; \alpha) &= 0. \end{aligned}$$

Let $0 < \varepsilon < 2M_f - R_i$. By Cauchy stability and monotonicity properties of Raychaudhuri's equation (4.2), there exists a $\delta > 0$ such that for every $0 < |\alpha| \leq \delta$,

$$\begin{aligned} \sup_{[0,1]} |r(\cdot; \alpha) - 2M_f| &\leq \varepsilon, \\ \inf_{[0,1]} \partial_v r(\cdot; \alpha) &\geq 0, \\ \partial_v r(0; \alpha) &> 0. \end{aligned}$$

The final inequality follows from the fact that $\alpha \neq 0$.

We now consider the sphere $S_\delta^k \doteq \{\alpha \in \mathbb{R}^{k+1} : |\alpha| = \delta\}$. For each $\alpha \in S_\delta^k$, define $D_\alpha(0) \in \mathcal{D}_k$ by setting

- $\varrho = r(0; \alpha) > 0$,
- $\varrho_v^1 = \partial_v r(0; \alpha) > 0$,
- $\varrho_u^1 = -\frac{1}{4}(\varrho_v^1)^{-1}$,
- $\omega = 1$, and
- all other components to zero.

By Lemma 4.1, $D_\alpha(0)$ is equivalent to $D_{r(0; \alpha), k}^M$ up to a gauge transformation.

For each $\alpha \in S_\delta^k$, we now apply Proposition 2.3 and Proposition 2.4 to uniquely determine cone data

$$D_\alpha : [0, 1] \rightarrow \mathcal{D}_k,$$

with initialization $D_\alpha(0)$ above and seed data ϕ_α given by (4.1). By standard ODE theory, $D_\alpha(v)$ is jointly continuous in v and α . Note that $\varrho(D_\alpha(v)) = r(v; \alpha)$ and $\varphi(D_\alpha(v)) = \phi(v; \alpha)$ by definition. We now use the notation

$$\partial_u^i \phi(v; \alpha) \doteq \varphi_u^i(D_\alpha(v))$$

for $i = 1, \dots, k$ to denote the transverse derivatives of the scalar field obtained by Proposition 2.3.

By construction, the data set $D_\alpha(1)$ satisfies

- $\varrho = 2M_f$,
- $\varrho_u^1 < 0$,
- $\varrho_v^1 = 0$,
- $\omega = 1$, and
- $\varphi_v^i = 0$ for $0 \leq i \leq k$.

The second property follows from the initialization of ϱ_u^1 in $D_\alpha(0)$ and the monotonicity of

$$(r \partial_u r)(v; \alpha) \doteq \varrho(D_\alpha(v)) \varrho_u^1(D_\alpha(v))$$

in the Einstein-scalar field system discussed in Remark 3.5.

In order to glue to Schwarzschild at $v = 1$, by Lemma 4.2, it suffices to find an $\alpha_* \in S_\delta^k$ for which additionally

$$\partial_u \phi(1; \alpha_*) = \dots = \partial_u^k \phi(1; \alpha_*) = 0.$$

The following discrete symmetry of the Einstein-scalar field system plays a decisive role in finding α_* .

A function $f(v; \alpha)$ is *even in α* if $f(v; -\alpha) = f(v; \alpha)$ and *odd in α* if $f(v; -\alpha) = -f(v; \alpha)$.

Lemma 4.3. *As functions on $[0, 1] \times S_\delta^k$, the metric coefficients $r(v; \alpha)$, $\Omega^2(v; \alpha)$ and all their ingoing and outgoing derivatives are even functions of α . The scalar field $\phi(v; \alpha)$ and all its ingoing and outgoing derivatives are odd functions of α . In particular, the map*

$$\begin{aligned} F : S_\delta^k &\rightarrow \mathbb{R}^k \\ \alpha &\mapsto (\partial_u \phi(1; \alpha), \dots, \partial_u^k \phi(1; \alpha)) \end{aligned} \tag{4.3}$$

is continuous and odd.

Proof. The scalar field itself is odd by the definition (4.1). Since Raychaudhuri's equation (4.2) involves the square of $\partial_v \phi(v; \alpha)$, $r(v; \alpha)$ will be automatically even. Next, $\partial_u r(v; \alpha)$ is found by integrating the wave equation for the radius (2.5), forwards in v with initial value determined by $D_\alpha(0)$. Since ϕ enters into this equation with an even power (namely zero), $\partial_u r(v; \alpha)$ will also be even. The wave equation for $r\phi$ in the Einstein-scalar field model can be derived from (2.13) and reads

$$\partial_u \partial_v (r\phi) = -\frac{\Omega^2 m}{2r^3} r\phi,$$

and the right-hand side is odd in α (the Hawking mass is constructed from metric coefficients so is also even). Recall from Proposition 2.3 that this wave equation is used to compute $\varphi_u^i(D_\alpha(v))$. By inspection $\partial_u(r\phi)$ is odd, whence $\partial_u \phi(v; \alpha)$ is also odd. The proof now follows by inductively following the procedure of Proposition 2.2, taking note of the fact that the transport equations for ingoing derivatives of r and Ω^2 only involve even powers of ϕ and its derivatives, whereas the transport equations for ingoing derivatives of ϕ only involve odd powers.

The claim about the map F follows from the oddness of ingoing derivatives of ϕ and the continuity of all dynamical quantities in α , per standard ODE theory. \square

We now complete the proof of Theorem 2A. By the Borsuk–Ulam theorem stated as Theorem 3, $F(\alpha_*) = 0$ for some $\alpha_* \in S_\delta^k$, where F is as in (4.3). By Lemma 4.2, $D_{\alpha_*}(1)$ is gauge equivalent to $D_{M_f, k}^S$.

So far we have glued $D_{r(0; \alpha), k}^M$ to $D_{M_f, k}^S$, and since $r(0; \alpha) > R_i$, we extend the data trivially in order to glue $D_{R_i, k}^M$ to $D_{M_f, k}^S$, which concludes the proof of Theorem 2A. \square

4.2 Proof of Theorem 2B

In this subsection we prove Theorem 2B. We assume that $\mathfrak{q} \neq 0$, the $\mathfrak{q} = 0$ version of this result being essentially a repeat of the arguments in the previous section combined with the new initialization of $\partial_u r(0; \alpha)$ in (4.17) below.

In this subsection we adopt the notational convention that $A \lesssim B$ means $A \leq CB$, where C is a constant that depends only on k and the baseline scalar field profile, but not on \mathfrak{q} , ϵ , M_i , M_f , or α . The notation $A \approx B$ means $A \lesssim B$ and $B \lesssim A$.

Let

$$0 = v_0 < v_1 < \cdots < v_{2k} < v_{2k+1} = 1$$

be an arbitrary partition of $[0, 1]$. For each $1 \leq j \leq 2k + 1$, fix a nontrivial bump function

$$\chi_j \in C_c^\infty((v_{j-1}, v_j); \mathbb{R}).$$

In the rest of this section, the functions $\chi_1, \dots, \chi_{2k+1}$ are fixed and our constructions depend on these choices.

For $\alpha = (\alpha_1, \dots, \alpha_{2k+1}) \in \mathbb{R}^{2k+1}$, set

$$\phi_\alpha(v) \doteq \phi(v; \alpha) \doteq \sum_{1 \leq j \leq 2k+1} \alpha_j \chi_j(v) e^{-iv}. \quad (4.4)$$

Remark 4.2. If $\epsilon > 0$, this choice of ϕ will make $Q \geq 0$, which is consistent with $\mathfrak{q} > 0$. If $\epsilon > 0$ and $\mathfrak{q} < 0$, then we replace $-iv$ in the exponential with $+iv$. Similarly, the cases $\epsilon < 0$, $\mathfrak{q} > 0$ and $\epsilon < 0$, $\mathfrak{q} < 0$ can be handled. Therefore, we assume without loss of generality that $\epsilon > 0$, $\mathfrak{q} > 0$.

For $\hat{\alpha} \in S^{2k}$ (the unit sphere in \mathbb{R}^{2k+1}) and $\beta \geq 0$, it is convenient to define $r(v; \beta, \hat{\alpha}) = r(v; \beta \hat{\alpha})$, etc. We again set $\Omega^2(v; \alpha) \equiv 1$ and study the equations (2.11) and (2.8) for $v \in [0, 1]$ with the ϕ_α ansatz:

$$\partial_v^2 r(v; \alpha) = -|\alpha|^2 r(v; \alpha) |\partial_v \phi_{\hat{\alpha}}(v)|^2, \quad (4.5)$$

$$\partial_v Q(v; \alpha) = \epsilon |\alpha|^2 r(v; \alpha)^2 \text{Im}(\phi_{\hat{\alpha}}(v) \overline{\partial_v \phi_{\hat{\alpha}}(v)}). \quad (4.6)$$

In addition, we again define r at $v = 1$ by

$$\begin{aligned} r(1; \alpha) &= r_+, \\ \partial_v r(1; \alpha) &= 0, \end{aligned}$$

and Q at $v = 0$ by

$$Q(0; \alpha) = 0, \tag{4.7}$$

which together with (4.5) and (4.6) uniquely determine r and Q on $[0, 1]$. Note that we will initialize $\partial_u r$ only later in (4.17).

We first note that basic calculations yield

$$|\partial_v \phi_{\hat{\alpha}}|^2 = \sum_{1 \leq j \leq 2k+1} \hat{\alpha}_j^2 (\chi_j^2 + \chi_j'^2)$$

and

$$\text{Im}(\phi_{\hat{\alpha}} \overline{\partial_v \phi_{\hat{\alpha}}}) = \sum_{1 \leq j \leq 2k+1} \hat{\alpha}_j^2 \chi_j^2.$$

Therefore,

$$\int_0^1 |\partial_v \phi_{\hat{\alpha}}|^2 dv \approx \int_0^1 \text{Im}(\phi_{\hat{\alpha}} \overline{\partial_v \phi_{\hat{\alpha}}}) dv \approx 1$$

for any $\hat{\alpha} \in S^{2k}$.

Lemma 4.4. *There exists a constant $0 < c \lesssim 1$ such that if $0 < \beta \leq c$, then for any $\hat{\alpha} \in S^{2k}$, $r(\cdot; \beta \hat{\alpha})$ satisfies*

$$r(v; \beta \hat{\alpha}) \geq \frac{1}{2} r_+ \tag{4.8}$$

$$\partial_v r(v; \beta \hat{\alpha}) \geq 0 \tag{4.9}$$

for $v \in [0, 1]$, where

$$r_+ \doteq (1 + \sqrt{1 - \mathfrak{q}^2}) M_f.$$

Furthermore,

$$\partial_v r(0; \beta \hat{\alpha}) > 0. \tag{4.10}$$

Proof. This is a simple bootstrap argument in v . Assume that on $[v_0, 1] \subset [0, 1]$, we have

$$\begin{aligned} \inf_{[v_0, 1]} r &\geq 0 \\ \inf_{[v_0, 1]} \partial_v r &\geq 0. \end{aligned}$$

This is clear for v_0 close to 1 by Cauchy stability. From Raychaudhuri's equation (4.5), $r \geq 0$ implies $\partial_v r$ is monotone decreasing, hence is bounded above by $\partial_v r(v_0)$, which can be estimated by

$$\partial_v r(v_0) = \int_{v_0}^1 \beta^2 r |\partial_v \phi_{\hat{\alpha}}|^2 dv \lesssim \beta^2 r_+, \tag{4.11}$$

since $r \leq r_+$ on $[v_0, 1]$. It follows that

$$r(v_0) = r_+ - \int_{v_0}^1 \partial_v r dv \geq r_+ - C \beta^2 r_+ \tag{4.12}$$

for some $C \lesssim 1$. Choosing $\beta > 0$ sufficiently small shows $r(v_0) \geq \frac{1}{2} r_+$ which improves the bootstrap assumptions and proves the desired estimate (4.8). Finally, note that (4.10) holds true as $\partial_v r$ is monotone decreasing and r is not constant ($\beta > 0$ and the scalar field is not identically zero). \square

Lemma 4.5. *By potentially making the constant c from Lemma 4.4 smaller, we have that for any $0 < \beta \leq c$ and $\hat{\alpha} \in S^{2k}$, the following estimate holds*

$$\frac{\partial}{\partial \beta} Q(1; \beta, \hat{\alpha}) > 0.$$

Proof. Integrating Maxwell's equation (4.6) and using (4.7), we find

$$Q(1; \beta, \hat{\alpha}) = \int_0^1 \mathfrak{e} \beta^2 r^2 \operatorname{Im}(\phi_{\hat{\alpha}} \overline{\partial_v \phi_{\hat{\alpha}}}) dv.$$

A direct computation yields

$$\partial_\beta Q(1; \beta, \hat{\alpha}) = 2\mathfrak{e} \beta \int_0^1 (r^2 + \beta r \partial_\beta r) \operatorname{Im}(\phi_{\hat{\alpha}} \overline{\partial_v \phi_{\hat{\alpha}}}) dv.$$

Note that $\operatorname{Im}(\phi_{\hat{\alpha}} \overline{\partial_v \phi_{\hat{\alpha}}}) \geq 0$ pointwise and is not identically zero. Since $0 < \beta \leq c$, we use Lemma 4.4 to estimate

$$r^2 + \beta r \partial_\beta r \geq \frac{1}{4} r_+^2 - C \beta r_+^2 = r_+^2 (\frac{1}{4} - C \beta),$$

where we also used $|\partial_\beta r| \lesssim r_+$ which follows directly from differentiating (4.5) with respect to $\beta = |\alpha|$. Therefore, by choosing c even smaller, we obtain $\partial_\beta Q(1; \beta, \hat{\alpha}) > 0$. \square

Lemma 4.6. *If $\mathfrak{e} M_f / \mathfrak{q}$ is sufficiently large depending only on k and the choice of profiles, then there is a smooth function $\beta_Q : S^{2k} \rightarrow (0, \infty)$ so that $Q(1; \beta_Q(\hat{\alpha}), \hat{\alpha}) = \mathfrak{q} M_f$ for every $\hat{\alpha} \in S^{2k}$, which also satisfies*

$$\beta_Q(\hat{\alpha}) \approx \frac{\sqrt{\mathfrak{q} M_f}}{\sqrt{\mathfrak{e} r_+}} \quad (4.13)$$

$$\beta_Q(-\hat{\alpha}) = \beta_Q(\hat{\alpha}) \quad (4.14)$$

for every $\hat{\alpha} \in S^{2k}$.

Proof. As in the proof of Lemma 4.5 we have

$$Q(1; \beta, \hat{\alpha}) = \mathfrak{e} \beta^2 \int_0^1 r^2 \operatorname{Im}(\phi_{\hat{\alpha}} \overline{\partial_v \phi_{\hat{\alpha}}}) dv.$$

If β is sufficiently small so that Lemma 4.4 and Lemma 4.5 apply, we estimate

$$Q(1; \beta, \hat{\alpha}) \approx \mathfrak{e} \beta^2 r_+^2.$$

For $\mathfrak{e} M_f / \mathfrak{q}$ sufficiently large as in the assumption, we apply now the intermediate value theorem, to obtain a $\beta_Q(\hat{\alpha})$ satisfying $0 < \beta_Q(\hat{\alpha}) \leq c$ such that

$$Q(1; \beta_Q, \hat{\alpha}) = \mathfrak{q} M_f. \quad (4.15)$$

Note that $\beta_Q(\hat{\alpha})$ is unique since $Q(1; \cdot, \hat{\alpha})$ is strictly increasing as shown in Lemma 4.5. Moreover, since $Q(1; \cdot, \cdot)$ is smooth (note that $\hat{\alpha} \in S^{2k}$ and $\beta > 0$ enter as smooth parameters in (4.6) which defines Q), a direct application of the implicit function theorem using that $\partial_\beta Q(1; \cdot, \hat{\alpha}) \neq 0$ shows that $\beta_Q : S^{2k} \rightarrow (0, \infty)$ is smooth.

Moreover, by (4.2) and (4.15), β_Q satisfies

$$\mathfrak{e} \beta_Q^2 r_+^2 \approx \mathfrak{q} M_f$$

which shows (4.13). Finally, note that $Q(1; \beta, -\hat{\alpha}) = Q(1; \beta, \hat{\alpha})$, from which (4.14) follows. \square

Lemma 4.7. *Let $\mathfrak{c}M_f/\mathfrak{q}$ be sufficiently large (depending only on k and the choice of profiles) so that Lemma 4.6 applies. Then*

$$\begin{aligned} p_Q : S^{2k} &\rightarrow \mathfrak{Q}^{2k} \\ \hat{\alpha} &\mapsto \beta_Q(\hat{\alpha})\hat{\alpha} \end{aligned}$$

is a diffeomorphism, where

$$\mathfrak{Q}^{2k} \doteq \{\beta_Q(\hat{\alpha})\hat{\alpha} : \hat{\alpha} \in S^{2k}\} \subset \mathbb{R}^{2k+1}$$

is the radial graph of β_Q . Moreover, \mathfrak{Q}^{2k} is invariant under the antipodal map $A(\alpha) = -\alpha$ and p_Q commutes with the antipodal map.

Proof. By definition of \mathfrak{Q}^{2k} and the facts that β_Q is smooth, positive, and invariant under the antipodal map as proved in Lemma 4.6, the stated properties of \mathfrak{Q}^{2k} and p_Q follow readily. \square

Having identified the set \mathfrak{Q}^{2k} which guarantees gluing of the charge Q , for the rest of the section we will always take $\alpha \in \mathfrak{Q}^{2k}$. Recall from (4.13) that for every $\alpha \in \mathfrak{Q}^{2k}$:

$$|\alpha| \approx \frac{\sqrt{\mathfrak{q}M_f}}{\sqrt{\mathfrak{c}r_+}}. \quad (4.16)$$

Before proceeding to choose sphere data, we will need to examine the equation for $\partial_u r$ because this will place a further restriction on α which must be taken into account before setting up the topological argument. We continue by using the definition of the Hawking mass m in (2.1), to impose the condition

$$m(0; \alpha) = M_i$$

by initializing

$$\partial_u r(0; \alpha) = - \left(1 - \frac{2M_i}{r(0; \alpha)}\right) \frac{1}{4\partial_v r(0; \alpha)}. \quad (4.17)$$

The transverse derivative $\partial_u r(v; \alpha)$ is now determined by solving (2.5),

$$\partial_v \partial_u r(v; \alpha) = -\frac{1}{4r(v; \alpha)^2} - \frac{\partial_u r(v; \alpha) \partial_v r(v; \alpha)}{r(v; \alpha)^2} + \frac{Q(v; \alpha)^2}{4r(v; \alpha)^3}, \quad (4.18)$$

with initialization (4.17).

Note that (4.17) is well-defined by (4.10) and (4.8) from Lemma 4.4. Furthermore,

$$1 - \frac{2M_i}{r(0; \alpha)} \geq 1 - \frac{4M_i}{M_f} > 0,$$

so

$$\partial_u r(0; \alpha) < 0. \quad (4.19)$$

Having initialized $\partial_u r$ at $v = 0$, we determine $\partial_u r(v; \alpha)$ using (4.18), and we will now show that for $\mathfrak{c}M_f/\mathfrak{q}$ sufficiently large, $\partial_u r(v; \alpha) < 0$ for all $v \in [0, 1]$.

Lemma 4.8. *If $\mathfrak{c}M_f/\mathfrak{q}$ is sufficiently large depending only on k and the choice of profiles and if $0 \leq M_i \leq \frac{1}{8}M_f$, then*

$$\sup_{v \in [0, 1]} \partial_u r(v; \alpha) < 0 \quad (4.20)$$

for every $\alpha \in \mathfrak{Q}^{2k}$.

Proof. Since $r > 0$ on $[0, 1]$, it suffices to show that

$$\sup_{[0, 1]} r \partial_u r < 0.$$

First, by (2.12),

$$|\partial_v(r\partial_u r)| = \left| \frac{1}{4} \left(1 - \frac{Q^2}{r^2} \right) \right| \lesssim 1, \quad (4.21)$$

as

$$Q(v; \alpha) \leq Q(1; \alpha) = \mathfrak{q}M_f \lesssim r(v; \alpha),$$

where we used (4.8). Integrating (4.21), we have

$$\sup_{v \in [0,1]} r(v) \partial_u r(v) \leq r(0) \partial_u r(0) + C_1, \quad (4.22)$$

where $C_1 \lesssim 1$ is a constant. Analogously to (4.11), we estimate

$$\partial_v r(0; \alpha) \lesssim |\alpha|^2 r_+ \lesssim \frac{\mathfrak{q}}{\mathfrak{e}},$$

where we used (4.16). Now, using (4.17),

$$\begin{aligned} -r(0) \partial_u r(0) &= \frac{r(0) - 2M_i}{4\partial_v r(0)} \\ &\gtrsim \frac{\mathfrak{e}}{\mathfrak{q}} \left(\frac{1}{2} M_f - 2M_i \right) \\ &\gtrsim \frac{\mathfrak{e}}{\mathfrak{q}} M_f. \end{aligned}$$

Therefore, we improve (4.22) to

$$\sup_{v \in [0,1]} r(v) \partial_u r(v) \leq -C_2 \frac{\mathfrak{e}}{\mathfrak{q}} M_f + C_1$$

for some $C_2 \lesssim 1$. Thus, if $\mathfrak{e}M_f/\mathfrak{q}$ is sufficiently large we obtain (4.20). \square

To continue the proof of Theorem 2B, we now put our construction into the framework of the sphere data in Section 3.3. For each $\alpha \in \mathfrak{Q}^{2k}$, define $D_\alpha(0) \in \mathcal{D}_k$ by setting

- $\varrho = r(0; \alpha) \geq \frac{1}{2}r_+$ (see (4.8)),
- $\varrho_v^1 = \partial_v r(0; \alpha) > 0$ (see (4.10)),
- $\varrho_u^1 = \partial_u r(0; \alpha) < 0$ (see (4.17) and (4.19)),
- $\omega = 1$, and
- all other components to zero.

By Lemma 4.1, $D_\alpha(0)$ is equivalent to $D_{M_i, r(0; \alpha), k}^S$ up to a gauge transformation.

For each $\alpha \in \mathfrak{Q}^{2k}$, we now apply Proposition 2.3 and Proposition 2.4 to uniquely determine cone data

$$D_\alpha : [0, 1] \rightarrow \mathcal{D}_k,$$

with initialization $D_\alpha(0)$ above and seed data ϕ_α given by (4.4). By standard ODE theory, $D_\alpha(v)$ is jointly continuous in v and α . Note that $\varrho(D_\alpha(v)) = r(v; \alpha)$, $\varphi(D_\alpha(v)) = \phi(v; \alpha)$, and $q(D_\alpha(v)) = Q(v; \alpha)$ by definition. As in the proof of Theorem 2A, we use the notation

$$\partial_u^i \phi(v; \alpha) \doteq \varphi_u^i(D_\alpha(v))$$

for $i = 1, \dots, k$ to denote the transverse derivatives of the scalar field obtained by Proposition 2.3. Note also that

$$\partial_u r(v; \alpha) = \varrho_u^1(D_\alpha(v)),$$

where $\partial_u r(v; \alpha)$ is as in (2.5) above.

By construction, the data set $D_\alpha(1)$ satisfies

- $\varrho = 2M_f$,
- $\varrho_u^1 < 0$ (see Lemma 4.8),
- $\varrho_v^1 = 0$,
- $\omega = 1$,
- $q = \mathfrak{q}M_f$ (definition of \mathfrak{Q}^{2k}), and
- $\varphi_v^i = 0$ for $0 \leq i \leq k$.

In order to glue to the appropriate Reissner–Nordström event horizon sphere, by Lemma 4.2, it suffices to find an $\alpha_* \in \mathfrak{Q}^{2k}$ for which additionally

$$\partial_u \phi(1; \alpha_*) = \cdots = \partial_u^k \phi(1; \alpha_*) = 0.$$

Analogously to Lemma 4.3 we first establish

Lemma 4.9. *The metric coefficients $r(v; \alpha)$, $\Omega^2(v; \alpha)$, the electromagnetic quantities $Q(v; \alpha)$, $A_u(v; \alpha)$, and all their ingoing and outgoing derivatives are even functions of α . The scalar field $\phi(v; \alpha)$ and all its ingoing and outgoing derivatives are odd functions of α .*

Proof. The proof is essentially the same as Lemma 4.3, noting that equations (2.7), (2.8), and (2.9) are also even in ϕ . \square

We now complete the proof of Theorem 2B. Recall from Lemma 4.7 that $p_Q : S^{2k} \rightarrow \mathfrak{Q}^{2k}$ is a diffeomorphism which commutes with the antipodal map. We now argue similarly to Section 4.1. By Lemma 4.9, the function

$$F : \mathfrak{Q}^{2k} \rightarrow \mathbb{C}^k$$

$$\alpha \mapsto (\partial_u \phi(1; \alpha), \dots, \partial_u^k \phi(1; \alpha))$$

is continuous and odd. Therefore, the Borsuk–Ulam theorem, stated as Theorem 3, applied to

$$(\operatorname{Re} F^1, \operatorname{Im} F^1, \dots, \operatorname{Re} F^k, \operatorname{Im} F^k) \circ p_Q : S^{2k} \rightarrow \mathbb{R}^{2k},$$

where F^i is the i th component of F , shows that there is an $\alpha_* \in \mathfrak{Q}^{2k}$ such that $F(\alpha_*) = 0$. By Lemma 4.2, $D_{\alpha_*}(1)$ is gauge equivalent to $D_{M_f, \mathfrak{q}M_f, k}^{\operatorname{RN}\mathcal{H}}$ which concludes the gluing construction. Since we have already established that $\partial_u r < 0$ for all $v \in [0, 1]$ in Lemma 4.8, this concludes the proof of Theorem 2B. \square

4.3 Proof of Theorem 2C

In this section we extend our characteristic gluing result Theorem 2B to allow for sphere data at the final sphere which is not necessarily located on a horizon. Recall Definition 3.5 for the definition of general Reissner–Nordström sphere data. As the steps in the proof below are direct generalizations of the proof of Theorem 2B, our presentation here will have fewer details.

Proof of Theorem 2C. We only consider the case $\mathfrak{q} \neq 0$, the case $\mathfrak{q} = 0$ being strictly easier and requiring only “gluing 3” below. Without loss of generality, we may also assume $R_f \leq 3M_f$ as for $r \geq 3M_f$ we can extend trivially with Reissner–Nordström data satisfying $\partial_v r > 0$ and $\partial_u r < 0$. In the following proof, we use the convention that all constants appearing in \lesssim, \gtrsim and \approx to also depend on $\mathfrak{q}, \mathfrak{r}$ and \mathfrak{e} . The theorem is proved as a consequence of the following three intermediate gluings:

1. $D_{R_i, k}^{\operatorname{M}}$ is glued to $D_{M', Q_f, R_1, k}^{\operatorname{RN}}$ with a complex scalar field,
2. $D_{M', Q_f, R_1, k}^{\operatorname{RN}}$ is glued to $D_{M', Q_f, R_2, k}^{\operatorname{RN}}$ trivially (i.e., with identically vanishing scalar field), and
3. $D_{M', Q_f, R_2, k}^{\operatorname{RN}}$ is glued to $D_{M_f, Q_f, R_f, k}^{\operatorname{RN}}$ with a real scalar field,

where $R_i \doteq R_f - M_f^{3/4}$, $0 < M' < M_f$ is an intermediate modified Hawking mass, $Q_f \doteq qM_f$, R_1, R_2 are intermediate radii which satisfy $R_i < R_1 < R_2$.

Gluing 1. In the interval $v \in [0, 1]$ we impose the ansatz (4.4). At $v = 0$, we set

$$r(0) = R_i, \quad m(0) = Q(0) = 0, \quad \partial_u r(0) = -\frac{1}{2M_f^{1/2}}, \quad \partial_v r(0) = \frac{M_f^{1/2}}{2}. \quad (4.23)$$

The pulse parameters α_* which achieve gluing of transverse derivatives of ϕ are determined by the procedure of Section 4.2, with charge condition $Q(1; \alpha) = Q_f$. As in Section 4.2 we find that the gluing can be performed with parameters satisfying $|\alpha_*|^2 \lesssim M_f^{-1}$. Using this estimate on α_* , we obtain from Raychaudhuri's equation (2.11) and (4.23) that $\frac{1}{2}M_f^{1/2} \geq \partial_v r \geq \frac{1}{4}M_f^{1/2}$ for every $v \in [0, 1]$ by choosing $M_0(k, q, \mathfrak{c}, \mathfrak{r})$ sufficiently large. This also implies $R_i \leq r \leq R_i + \frac{1}{2}M_f^{1/2}$. Using $r \geq R_f - M_f^{3/4}$ and the estimate analogous to (4.21) we infer $|r\partial_u r - r(0)\partial_u r(0)| \lesssim 1$ for every $v \in [0, 1]$, i.e., $0 < -\partial_u r \leq M_f^{-1/2}$. We now estimate the Hawking mass at $v = 1$ by integrating (2.14),

$$m(1) = \int_0^1 2r^2(-\partial_u r)|\partial_v \phi|^2 dv + \int_0^1 \frac{Q^2}{2r^2} \partial_v r dv \lesssim M_f^2 M_f^{-1/2} M_f^{-1} + M_f^{1/2} \lesssim M_f^{1/2}. \quad (4.24)$$

Setting $R_1 = r(1)$ and $M' = m(1) + Q_f^2/(2R_1)$, we have shown that $R_i < R_1 \leq R_i + \frac{1}{2}M_f^{1/2}$. The condition (3.2) shows that $Q_f^2/(2R_f) \leq M_f/(1 + \mathfrak{r})$. In particular, since $R_1 \geq R_f - M_f^{3/4}$ we estimate

$$M' = m(1) + \frac{Q_f^2}{2R_1} \leq \frac{1}{2} \left(1 + \frac{1}{1 + \mathfrak{r}} \right) M_f = \frac{2 + \mathfrak{r}}{2 + 2\mathfrak{r}} M_f \quad (4.25)$$

by possibly taking $M_0(k, q, \mathfrak{c}, \mathfrak{r})$ larger. This completes the first gluing step.

Gluing 3. It is more convenient to now carry out the third gluing step and simply ensure that $R_2 > R_1$. We use a collection of $k + 1$ real-valued pulses as in (4.1) on $v \in [0, 1]$. We impose

$$r(1) = R_f, \quad \partial_u r(1) = -M_f, \quad Q(1) = Q_f, \quad \varpi(1) = M_f. \quad (4.26)$$

This uniquely determines $\partial_v r(1)$ which can have either sign but satisfies $|\partial_v r(1)| \lesssim M_f^{-1}$. We also note that as long as $|\alpha|^2 \leq M_f^{-3/2}$, we have $|\partial_v r| \lesssim M_f^{-1/2}$ and thus $|r - R_f| \lesssim M_f^{-1/2}$ on $[0, 1]$. This also gives $-\partial_u r \approx M_f$. Using

$$\varpi(1) - \varpi(0) = \int_0^1 2r^2(-\partial_u r)|\partial_v \phi|^2 dv$$

and (4.25), we write the mass condition $\varpi(1) = M_f$ and $\varpi(0) = M'$ as a sphere of α 's ($|\alpha|^2 \approx M_f^{-2}$) for which we will apply the Borsuk–Ulam argument. We use here that $M_f - M' = M_f \mathfrak{r}/(2 + 2\mathfrak{r})$. With $|\alpha_*|^2 \approx M_f^{-2}$ we have the improved estimate $|\partial_v r| \lesssim M_f^{-1}$ for $v \in [0, 1]$ and thus, $|r(0) - R_f| \lesssim M_f^{-1}$. Taking now $M_0(k, q, \mathfrak{c}, \mathfrak{r})$ sufficiently large makes $R_2 \doteq r(0) > R_1$.

Gluing 2. By the previous constructions, we have $R_1 < R_2$, $\varpi(0) = \varpi(1) = M'$, $Q(0) = Q(1) = Q_f$, $\partial_v r(0) > 0$, and $\partial_u r(0) < 0$. Now $D_{M', Q_f, R_k}^{\text{RN}}$ can be trivially glued to $D_{M', Q_f, R_2, k}^{\text{RN}}$ by choosing $\phi \equiv 0$, and we must merely ensure that $\partial_u r < 0$ along the way. Since $\partial_v r > 0$ by Raychaudhuri's equation, this amounts to proving $\frac{2m}{r} < 1$. Indeed,

$$m(v) \leq m(0) + \int_0^1 \frac{Q_f^2}{2r^2} \partial_v r dv = m(0) + \int_{R_1}^{R_2} \frac{Q_f^2}{2r^2} dr \lesssim m(0) + (R_2 - R_1) \lesssim M_f^{1/2} + M_f^{3/4},$$

where we used (4.24). In particular, by choosing $M_0(k, q, \mathfrak{c}, \mathfrak{r})$ larger, we can make $m(v)/M_f$ arbitrarily small and thus $\partial_u r < 0$ throughout gluing 2. \square

5 Constructing the spacetimes and Cauchy data

In this final section we will prove our main result Theorem 1 as well as Corollary 1, Corollary 2, and Corollary 3.

5.1 Maximal future developments of asymptotically flat data for EMCSF

Our theorems and corollaries in this paper are stated in the framework of the Cauchy problem for the Einstein–Maxwell–charged scalar field system. We recall that Cauchy data for the EMCSF system consist of the usual Cauchy data (Σ, g_0, k_0) for the Einstein equations, where Σ is a 3-manifold, g_0 a Riemannian metric on Σ , and k_0 a symmetric 2-tensor field, together with initial data for the matter fields, namely initial electric and magnetic fields, E_0 and B_0 , and finally the scalar field ϕ_0 and its “time derivative” ϕ_1 . (See e.g. [Cho09, Section VI.10] for a treatment of the Einstein–Maxwell Cauchy problem.) Associated to a Cauchy data set is a unique maximal future globally hyperbolic development $(\mathcal{M}^4, g, F, A, \phi)$ [Fou52; CG69]. If the Cauchy data are moreover spherically symmetric, then the maximal development will be spherically symmetric by uniqueness.

We will not, however, actually construct our spacetimes by directly evolving Cauchy data. Rather, we construct the spacetimes *teleologically* by gluing together explicit spacetimes with the help of our characteristic gluing results and Proposition 3.1. In each case, a Cauchy hypersurface Σ is then found, within the spacetime, whose future domain of dependence contains the physically relevant region, and contains no anti-trapped spheres. At this point, all attention is restricted to this future domain of dependence. *A posteriori*, by the existence and uniqueness theory for the maximal globally hyperbolic development, the spacetime will then be contained in the maximal development of the induced data on the Cauchy hypersurface Σ .

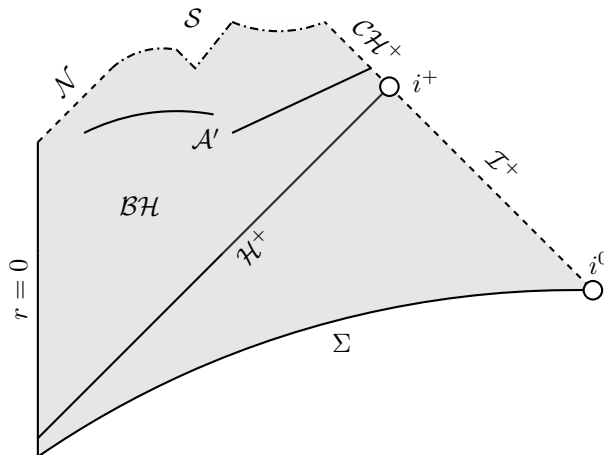


Figure 10: General structure of the MFGHD of asymptotically flat Cauchy data Σ in the EMCSF system in spherical symmetry [Kom13]. What is depicted is the quotient manifold \mathcal{Q} as a bounded subset of $\mathbb{R}_{u,v}^{1+1}$ with boundary suitably labeled. Note that various components of the diagram can be empty.

Since our examples are maximal globally hyperbolic developments of asymptotically flat, spherically symmetric Cauchy data for the EMCSF system with no antitrapped spheres of symmetry, we can make use of a general characterization of the boundary of spacetime in this context appearing in [Kom13]. In particular one can rigorously associate a global Penrose diagram, and unambiguously identify a nonempty null boundary component *future null infinity* \mathcal{I}^+ , *domain of outer communication* $J^-(\mathcal{I}^+)$, (possibly empty) *black hole region* $\mathcal{BH} \doteq \mathcal{M} \setminus J^-(\mathcal{I}^+)$, (possibly empty) *event horizon* $\mathcal{H}^+ \doteq \partial(\mathcal{BH})$, (possibly empty) *Cauchy horizon* \mathcal{CH}^+ , (possibly empty) $r = 0$ singularity \mathcal{S} , and (possibly empty) null boundary component \mathcal{N} emanating from a (possibly absent) “locally naked” singularity at the center. The Penrose diagram $\mathcal{Q} \subset \mathbb{R}_{u,v}^{1+1}$ can be viewed as a global double null chart for the spacetime, with v the “outgoing” null coordinate and u the “ingoing” coordinate. See Fig. 10.⁶

For use in the statement and proof of Theorem 1 below, we recall that in the EMCSF system in spherical

⁶Note that the above general boundary decomposition in particular proves that one cannot form a globally naked singularity once a marginally trapped surface has developed in the spacetime, which already rules out naked singularity formation by supercharging a black hole in spherical symmetry, see [Kom13, Section 1.9]. It is thus not at all surprising that ongoing numerical searches for these continue to be futile.

symmetry, the *apparent horizon* is defined by

$$\mathcal{A} \doteq \{\partial_v r = 0\} \subset \mathcal{BH}.$$

Since \mathcal{A} might have a complicated structure (in particular, it might have nonempty interior), we define an appropriate notion of boundary as follows. The *outermost apparent horizon* \mathcal{A}' consists of those points $p \in \mathcal{A}$ whose past-directed ingoing null segment lies in the strictly untrapped region $\{\partial_v r > 0\}$ and eventually exits the black hole region, i.e., enters $J^-(\mathcal{I}^+)$. \mathcal{A}' is a possibly disconnected achronal curve in the $(1+1)$ -dimensional reduction \mathcal{Q} of \mathcal{M} . Note, as depicted in Fig. 10, that \mathcal{A}' does not necessarily asymptote to future timelike infinity i^+ .

For definiteness, we will make extensive use of these notions in our theorems and corollaries. However, our notation and usage should be sufficiently familiar to readers acquainted with standard concepts in general relativity so that they may read our diagrams and understand our theorems without specific reference to [Kom13].

We also note that when referring to spherically symmetric subsets of (\mathcal{M}, g) , such as the event horizon \mathcal{H}^+ , we may view them as objects in \mathcal{M} or in the reduced space \mathcal{Q} . The context will make it clear which point of view we are taking.

Remark 5.1. In Appendix B, we show by a barrier argument that since $\partial_u r < 0$ in a spacetime satisfying the hypotheses of [Kom13], there are also no nonspherically symmetric antitrapped surfaces.

5.2 Construction of gravitational collapse to Reissner–Nordström

We now state a more precise version of Corollary 1 as follows.

Corollary 1. *For any $k \in \mathbb{N}$, $\mathfrak{q} \in [-1, 1] \setminus \{0\}$, and $\mathfrak{e} \in \mathbb{R} \setminus \{0\}$, let $M_0(k, \mathfrak{q}, \mathfrak{e})$ be as in Theorem 2B. Then for any $M \geq M_0$ there exist asymptotically flat, spherically symmetric Cauchy data $(\Sigma, g_0, k_0, E_0, B_0, \phi_0, \phi_1)$ for the EMCSF system, with $\Sigma \cong \mathbb{R}^3$ and a regular center, such that the maximal future globally hyperbolic development $(\mathcal{M}^4, g, F, A, \phi)$ has the following properties:*

- *All dynamical quantities are at least C^k -regular.*
- *Null infinity \mathcal{I}^+ is complete.*
- *The black hole region is nonempty, $\mathcal{BH} \doteq \mathcal{M} \setminus J^-(\mathcal{I}^+) \neq \emptyset$.*
- *The Cauchy surface Σ lies in the domain of outer communication $J^-(\mathcal{I}^+)$. In particular, it does not intersect the event horizon $\mathcal{H}^+ \doteq \partial(\mathcal{BH})$.*
- *The initial data hypersurface does not contain trapped surfaces.*
- *The spacetime does not contain antitrapped surfaces.*
- *For sufficiently late advanced times $v \geq v_0$, the domain of outer communication, including the event horizon, is isometric to that of a Reissner–Nordström solution with mass M charge to mass ratio \mathfrak{q} . For $v \geq v_0$, the event horizon of the spacetime can be identified with the event horizon of Reissner–Nordström.*

Remark 5.2. A similar statement can be made with $\mathfrak{q} = 0$ for the Einstein-scalar field model, using instead Theorem 2A. In that case, there will also be no assumption made on the mass.

Proof. We refer the reader to Fig. 11 for a visual guide to the proof. Using Theorem 2B with regularity index $k+1$ (see footnote below) and Proposition 3.1, a portion of Minkowski space

$$\begin{aligned} t + r &\leq \frac{1}{2}M, \\ t - r &\geq -\frac{1}{2}M, \end{aligned}$$

can be glued to a Reissner–Nordström solution with parameters M and $\mathfrak{q}M$. Note that as depicted, one can solve for a complete future neighborhood of the event horizon, which might not be a complete double null neighborhood.

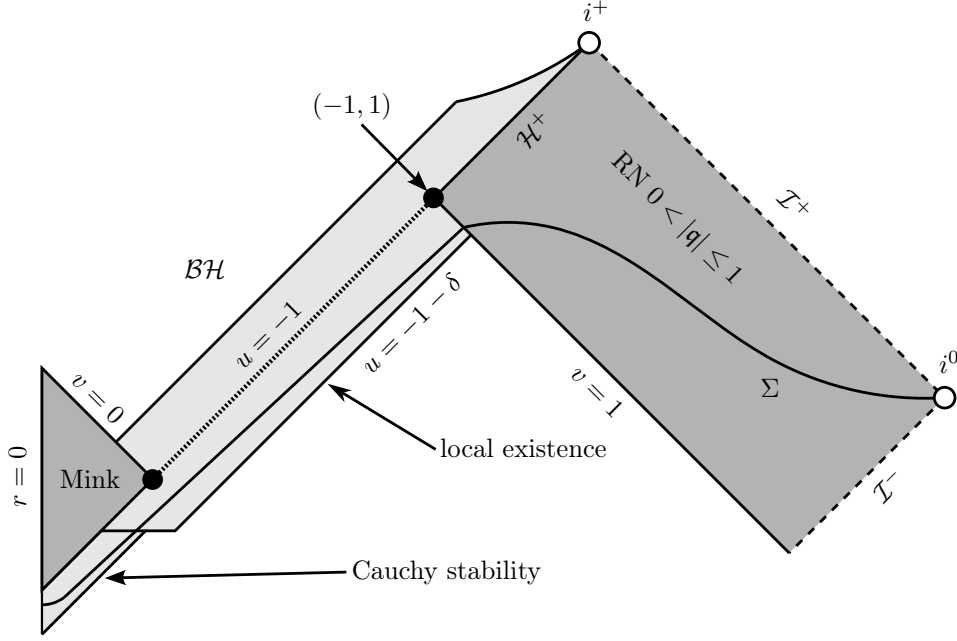


Figure 11: Penrose diagram for the proof of Corollary 1.

Since we are in spherical symmetry, standard techniques (see [Chr93, Section 5] or [LOY18, Section 3]) allow the “local existence” region emanating from the Reissner–Nordström portion of the spacetime to be extended all the way up to the center.⁷ (In this figure, this region is denoted “Cauchy stability” for reasons that will become clear below.)

We now identify a spacelike curve Σ connecting spacelike infinity i^0 in the exactly Reissner–Nordström region to the center, to the past of the cone $u = -1$. The curve Σ can be chosen so the induced data on it is asymptotically flat near i^0 . For example, it may be taken to be a constant t curve near i^0 in standard coordinates. Furthermore, by having Σ hug the gluing region closely enough, we are guaranteed to have no spherically symmetric antitrapped surfaces on Σ .

Completeness of null infinity \mathcal{I}^+ is inherited from the exact Reissner–Nordström solution. By inspecting Fig. 11, we see that the null hypersurface C_{-1} is the event horizon $\mathcal{H}^+ = \partial J^-(\mathcal{I}^+)$ of the spacetime and that Σ can be arranged to lie in the domain of outer communication $J^-(\mathcal{I}^+)$. The statement about trapped surfaces follows from Proposition B.2 below.

We now consider the (unique) maximal future globally hyperbolic development $(\mathcal{M}^4, g, F, A, \phi)$ of the induced data $(\Sigma, g_0, k_0, E_0, B_0, \phi_0, \phi_1)$ on Σ . By uniqueness of the MFGHD, it contains the domain of dependence of Σ in the gluing spacetime (and thus all shaded regions to the future of Σ in Fig. 11). Therefore, by construction, $(\mathcal{M}^4, g, F, A, \phi)$ has all the properties listed in the statement of Corollary 1. Note that the property of having no antitrapped symmetry spheres is propagated to the whole development by Raychaudhuri’s equation (2.10). By Proposition B.2, the spacetime does not contain any nonspherically symmetric antitrapped surfaces either. This concludes the proof. \square

The above proof made use of spherical symmetry in the local existence region and the region up to the center. In view of potentially extending our work to the Einstein vacuum equations in the future, we give a second construction of these regions which does not invoke spherical symmetry. First, the “local existence region” can be constructed outside of spherical symmetry by the well-known theorem of Luk [Luk12]. Once such a region has been constructed, we can use the fact that it lies “outside” of a Minkowski region to construct the rest of the spacetime, up to the center, by Cauchy stability:

Lemma 5.1. *Let B_{r_0} and B_{r_1} denote the (open) balls of radii $r_0 > 0$ and $r_1 > r_0$ in \mathbb{R}^3 , respectively. Consider on B_{r_1} data for the Einstein–Maxwell–charged scalar field system corresponding to Minkowski space,*

⁷The wave equation in spherical symmetry loses one derivative at the center when compared to characteristic data. Therefore, to obtain a globally C^k solution, we take C^{k+1} characteristic data.

$(\delta, 0, 0, 0, 0, 0)$. Let $D \doteq (g_0, k_0, E_0, B_0, \phi_0, \phi_1)$ be a C^k (for $k \in \mathbb{N}$ sufficiently large and not assumed to be spherically symmetric) initial data set for the Einstein–Maxwell-charged scalar field system defined on B_{r_1} which agrees with the Minkowski data set on B_{r_0} . Then the maximal globally hyperbolic development of D contains the Minkowski cone over B_{r_0} “in its interior” in the following sense:

There exists an $\varepsilon > 0$ and a development (g, F, A, ϕ) of the data D on $K_{r_0+\varepsilon} \doteq \{t+r < r_0+\varepsilon\} \cap \{t \geq 0\} \subset \mathbb{R}^{3+1}$ so that the development of the Minkowski portion of the data is defined on $K_{r_0} \doteq \{t+r < r_0\} \cap \{t \geq 0\}$ and is the Minkowski metric in those coordinates.

Proof. Since this is a standard Cauchy stability argument we merely sketch the proof. For $0 < \varepsilon < \frac{r_1-r_0}{2}$, let θ_ε be a cutoff function which is equal to one on $B_{r_0+\varepsilon}$ and vanishes outside $B_{r_0+2\varepsilon}$. On B_{r_1} , we consider the “initial data set”

$$D_\varepsilon \doteq (\theta_\varepsilon g_0 + (1 - \theta_\varepsilon)\delta, \theta_\varepsilon k_0, \theta_\varepsilon E_0, \theta_\varepsilon B_0, \theta_\varepsilon \phi_0, \theta_\varepsilon \phi_1).$$

This does not solve the constraints everywhere, but it does solve them on $B_{r_0+\varepsilon}$, where it equals D . We assume that $k \geq 5$ and show that D_ε is $O(\varepsilon)$ -close to the Minkowski data set in H^4 . Then Cauchy stability for the reduced Einstein equations (in harmonic coordinates) will show that a solution to the reduced equations with data D_ε exists on $K_{r_0+2\varepsilon}$ for ε sufficiently small. By domain of dependence arguments, a genuine solution will then exist on a smaller domain which still contains the entirety of $\overline{K_{r_0}}$ in its interior.

To show that D_ε is close to Minkowski data we must check it componentwise. For brevity, we only check $\theta_\varepsilon k_0$. Note first that

$$\|\theta_\varepsilon k_0\|_{H^4} \lesssim \|\theta_\varepsilon k_0\|_{C^4}.$$

Now since k_0 vanishes on B_{r_0} and is at least C^5 , Taylor’s theorem implies

$$|\partial_r^i \nabla^j k_0| \lesssim \max\{0, r - r_0\}^{5-i-j},$$

if $0 \leq i+j \leq 5$. In the region where either θ_ε or $\partial_r \theta_\varepsilon$ are nonvanishing, $\max\{0, r - r_0\} \lesssim \varepsilon$. It follows that

$$\|\theta_\varepsilon k_0\|_{H^4} \lesssim \sum_{0 \leq i+j \leq 4} \sup_{B_{r_1}} |\partial_r^i \nabla^j (\theta_\varepsilon k_0)| \lesssim \varepsilon,$$

which proves the claim and hence the lemma. \square

5.3 Construction of counterexample to the third law

In this section we prove Theorem 1 with an analogous approach as in the proof of Corollary 1. We first restate the result in more detail.

Theorem 1. *For any $k \in \mathbb{N}$ and $\mathfrak{c} \in \mathbb{R} \setminus \{0\}$, there exist asymptotically flat, spherically symmetric Cauchy data $(\Sigma, g_0, k_0, E_0, B_0, \phi_0, \phi_1)$, with $\Sigma \cong \mathbb{R}^3$ and a regular center, for the EMCSF system such that the maximal future globally hyperbolic development $(\mathcal{M}^4, g, F, A, \phi)$ has the following properties:*

- All dynamical quantities are at least C^k -regular.
- The spacetime and Cauchy data satisfy all the conclusions of Corollary 1 with $\mathfrak{q} = 1$ and final mass $M_f \geq M_0(1, \mathfrak{c}, k) + 8$.
- The spacetime contains a double null rectangle of the form $\mathfrak{R} \doteq \{-2 \leq u \leq -1\} \cap \{1 \leq v \leq 2\}$ which is isometric to a double null rectangle in a Schwarzschild spacetime of mass 1.
- The cone $\{u = -1\} \cap \mathfrak{R}$ lies in the outermost apparent horizon \mathcal{A}' of the spacetime and is isometric to an appropriate portion of the $r = 2$ hypersurface in the Schwarzschild spacetime of mass 1.
- The outermost apparent horizon \mathcal{A}' is disconnected.
- The spacetime contains trapped surfaces in the black hole region, for all arbitrarily late advanced time. More precisely, for every symmetry sphere $S_{u,v} \subset \mathcal{H}^+$, $J^+(S_{u,v})$ contains a trapped sphere.
- There exists a neighborhood \mathcal{U} of \mathcal{H}^+ in \mathcal{M} such that there are no trapped surfaces $S \subset \mathcal{U}$.

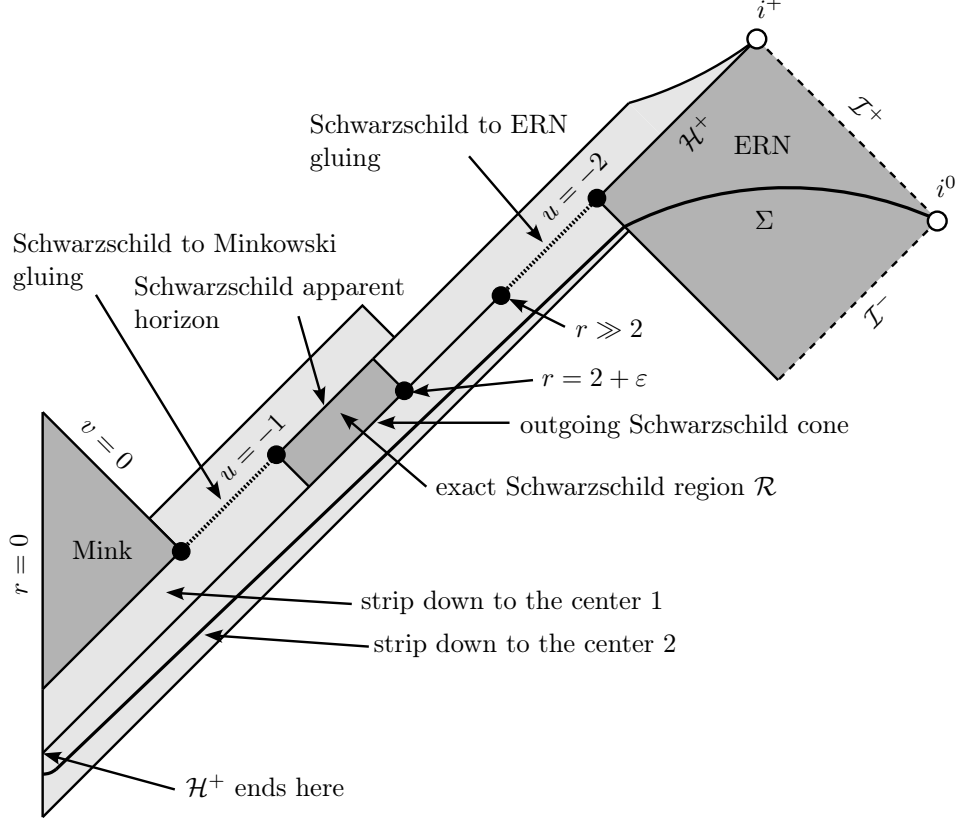


Figure 12: Penrose diagram for the proof of Theorem 1.

Proof. We refer to Fig. 12 for a Penrose diagram illustrating the proof. The proof begins as the proof of Corollary 1 (recall also Proposition 3.1), by gluing a Minkowski cone to a Schwarzschild event horizon of unit mass along $\{u = -1\}$. Then, attach a double null rectangle \mathfrak{R} of Schwarzschild along the hypersurface $r = 2$, as in Corollary 1, but stop after a finite advanced time $v = 2$. Now place $u = -2$ so that

$$\sup_{\{u=-2\} \cap \mathfrak{R}} r = 2 + \varepsilon \leq 3.$$

For ε sufficiently small, the first strip down to the center can be constructed as in the proof of Corollary 1. Now let $M_f \geq M_0 + 8$ and extend the cone $u = -2$ to the future with trivial scalar field until $r = \frac{1}{2}(M_0 + 8) \gg 3$. Then using Theorem 2B, extremal Reissner–Nordström of mass M_f can be attached. We again solve backward up to the center as in Corollary 1 and have now constructed the spacetime depicted in Fig. 12.

As in the proof of Corollary 1, we again find an asymptotically flat spacelike curve Σ connecting i^0 with the center and lying entirely in $J^-(\mathcal{I}^+)$. The maximal future globally hyperbolic development $(\mathcal{M}, g, F, A, \phi)$ of the induced data on Σ contains the domain of dependence of Σ in the spacetime constructed above (and thus all shaded regions to the future of Σ in Fig. 12) and satisfies all the conclusions of Corollary 1 with $q = 1$ and final mass $M_f \geq M_0(1, \mathfrak{e}, k) + 8$. By construction, \mathcal{M} contains the double null rectangle \mathfrak{R} which satisfies the stated properties. Further, the cone $\{u = -1\} \cap \mathfrak{R}$ lies in the apparent horizon \mathcal{A} of (\mathcal{M}, g) and $\{u = -1\} \cap \mathfrak{R}$ is isometric to an appropriate portion of the $r = 2$ hypersurface in the Schwarzschild spacetime of mass 1.

We readily see that (\mathcal{M}, g) contains trapped surfaces in any (future) neighborhood of $\{u = -1\} \cap \mathfrak{R}$ as $\partial_v r = 0$ along $\{u = -1\} \cap \mathfrak{R}$ and (2.12) evaluated on $\{u = -1\} \cap \mathfrak{R}$ gives

$$\partial_u(r\partial_v r) = -\frac{\Omega^2}{4}.$$

To prove that trapped surfaces exist for arbitrarily late advanced time, we invoke the general boundary

characterization of [Kom13]. If the $r = 0$ singularity \mathcal{S} is empty, then the outgoing cone starting from one of these trapped spheres terminates on the Cauchy horizon \mathcal{CH}^+ and the claim is clearly true by Raychaudhuri's equation (2.11). If \mathcal{S} is nonempty, then every outgoing null cone which terminates on \mathcal{S} is eventually trapped since r extends continuously by zero on \mathcal{S} . Furthermore, \mathcal{S} terminates at the Cauchy horizon \mathcal{CH}^+ or future timelike infinity i^+ , so the claim is also true in this case.

We now show that there exists a neighborhood \mathcal{U} of \mathcal{H}^+ in \mathcal{M} which does not contain *spherically symmetric* trapped surfaces. It suffices to show that there is a neighborhood \mathcal{V} of \mathcal{H}^+ in \mathcal{Q} such that $\partial_v r > 0$ on $\mathcal{V} \setminus \mathcal{H}^+$, where we use the same symbol for the event horizon in \mathcal{M} and \mathcal{Q} . Let $p \in \mathcal{H}^+$ be any sphere after the final gluing sphere, see Fig. 12. Then $r(p) = Q(p) = M_f$, $\partial_v r(p) = 0$, and $\phi(p) = 0$. Reparametrize the double null gauge so that $\Omega \equiv 1$ on the ingoing cone \underline{C} passing through p . By the wave equation for the radius (2.5),

$$\partial_u \partial_v r(p) = -\frac{1}{4M_f} + \frac{M_f^2}{4M_f^3} = 0.$$

Differentiating (2.5) in u , we find

$$\partial_u^2 \partial_v r = \frac{\partial_u r}{4r^2} - \partial_u (\partial_u \log r) \partial_v r - (\partial_u \log r) \partial_u \partial_v r - \frac{3Q^2 \partial_u r}{4r^4} + \frac{Q \partial_u Q}{2r^3}.$$

Evaluating at p , we find $\partial_u Q(p) = 0$ by Maxwell's equation (2.7), so we have

$$\partial_u^2 \partial_v r(p) = \frac{\partial_u r(p)}{4M_f^2} - \frac{3M_f^2 \partial_u r(p)}{4M_f^4} = -\frac{2\partial_u r(p)}{M_f^2} > 0.$$

Therefore, $\partial_v r$ becomes immediately positive for all points along \underline{C} sufficiently close to the event horizon but not on it (see also Fig. 5).⁸

By the monotonicity of Raychaudhuri's equation (2.11) and since $p \in \mathcal{H}^+$ after the final gluing sphere was arbitrary, this shows that there exists a neighborhood \mathcal{V} of \mathcal{H}^+ contained in \mathcal{Q} that does not contain trapped symmetry spheres except for \mathcal{H}^+ itself. That there are also no nonspherically symmetric trapped surfaces in $\mathcal{U} \doteq \mathcal{V} \times S^2$ now follows immediately from Proposition B.1 below.

The claim about the disconnectedness of the outermost apparent horizon \mathcal{A}' now follows from the fact that $\mathcal{A}' \cap \mathcal{H}^+$ is one connected component of \mathcal{A}' which does not contain $\{u = -1\} \cap \mathfrak{R} \subset \mathcal{A}'$. This concludes the proof. \square

5.4 Construction of collapse to Reissner–Nordström with piece of Cauchy horizon

In this section, we show that a mild modification of the proof of Corollary 1 allows us to construct examples of gravitational collapse such that the black hole region admits a piece of future boundary which is a Cauchy horizon which is isometric to a subextremal or extremal Reissner–Nordström Cauchy horizon.

Corollary 2. *For any $k \in \mathbb{N}$, $\mathbf{q} \in [-1, 1] \setminus \{0\}$, and $\mathbf{c} \in \mathbb{R} \setminus \{0\}$, let $M_0(k, \mathbf{q}, \mathbf{c}, 1/2)$ be as in Theorem 2C. Then for any $M \geq M_0$ there exist asymptotically flat, spherically symmetric Cauchy data $(\Sigma, g_0, k_0, E_0, B_0, \phi_0, \phi_1)$, with $\Sigma \cong \mathbb{R}^3$ and a regular center, for the EMCSF system such that the maximal future globally hyperbolic development $(\mathcal{M}^4, g, F, A, \phi)$ has the following properties:*

- All dynamical quantities are at least C^k -regular.
- The spacetime and Cauchy data satisfy all the conclusions of Corollary 1.
- The black hole region contains an isometrically embedded portion of a Reissner–Nordström Cauchy horizon neighborhood with parameters M and $\mathbf{q}M$, in particular $\mathcal{CH}^+ \neq \emptyset$.

⁸This calculation is related to the discussion in Section 1.4.6 above and Appendix A below. In fact, we have effectively just proved the claim in Remark A.1.

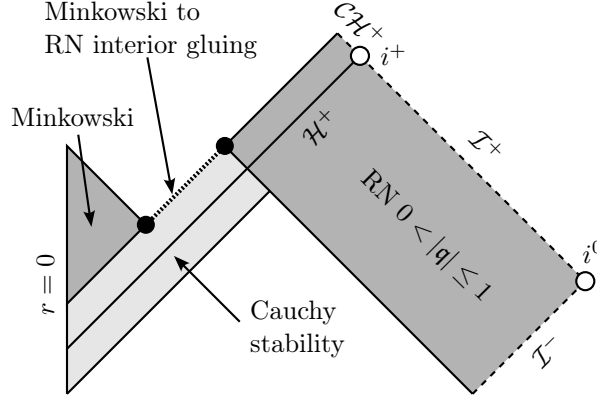


Figure 13: Penrose diagram depicting the proof of Corollary 2.

Proof. The proof is completely analogous to the proof of Corollary 1. We apply the gluing construction of Theorem 2C to glue a sphere in Minkowski space to a Reissner–Nordström interior sphere with radius $R_f < r_+$ and $r_+ - R_f$ small. Indeed, this can be achieved by setting $\mathfrak{r} = \frac{1}{2}$ in Theorem 2C as then $\frac{1}{2}M_f(1 + \mathfrak{r})\mathfrak{q}^2 \leq \frac{3}{4}M_f < M_f \leq r_+$. We then apply the local existence and Cauchy stability argument as in the proof of Corollary 1. We note that the u -width of the local existence and Cauchy stability argument remains uniform as $R_f \rightarrow r_+$ so by choosing R_f sufficiently close to r_+ , we guarantee that we find a Cauchy hypersurface Σ which does not intersect the event horizon. We refer to Fig. 13 for the Penrose diagram explaining the proof. \square

Remark 5.3. As in Remark 5.2, we note that a similar statement with a piece of Schwarzschild interior including the $\{r = 0\}$ singularity can be made with $\mathfrak{q} = 0$.

5.5 Construction of black hole interior for which the Cauchy horizon closes off spacetime

We now give our construction of a spacetime for which the Cauchy horizon closes off the black hole region.

Corollary 3. *For any $k \in \mathbb{N}$, $\mathfrak{q} \in [-1, 1] \setminus \{0\}$, $\mathfrak{e} \in \mathbb{R} \setminus \{0\}$, let $\tilde{M}_0(k, \mathfrak{q}, \mathfrak{e}, \mathfrak{q}^2/4)$ be as in Theorem 2C'. Then for any $M \geq \tilde{M}_0$ there exist asymptotically flat, spherically symmetric Cauchy data $(\Sigma, g_0, k_0, E_0, B_0, \phi_0, \phi_1)$, with $\Sigma \cong \mathbb{R}^3$ and a regular center, for the EMCSF system such that the maximal future globally hyperbolic development $(\mathcal{M}^4, g, F, A, \phi)$ has the following properties:*

- All dynamical quantities are at least C^k -regular.
- The spacetime does not contain antitrapped surfaces.
- The black hole region is nonempty, $\mathcal{BH} \doteq \mathcal{M} \setminus J^-(\mathcal{I}^+) \neq \emptyset$.
- The future boundary of the black hole region is a C^k -regular Cauchy horizon \mathcal{CH}^+ which closes off spacetime, i.e., $\mathcal{N} \cup \mathcal{S} = \emptyset$ in Fig. 10.
- The exterior region is isometric to a Reissner–Nordström exterior with mass M and charge $\mathfrak{q}M$. In particular, future null infinity \mathcal{I}^+ is complete.

Proof. Analogous to the proof of Corollary 2 we glue a Reissner–Nordström interior sphere with $R_f < r_-$ and $r_- - R_f$ small to a sphere in Minkowski space along an *ingoing* cone using Theorem 2C'. We can choose R_f arbitrarily close to r_- in Theorem 2C' by setting $\mathfrak{r} = \mathfrak{q}^2/4$. Indeed, in this case

$$r_- - \frac{M_f}{2} \left(1 + \frac{\mathfrak{q}^2}{4}\right) \mathfrak{q}^2 = M_f \left(1 - \sqrt{1 - \mathfrak{q}^2}\right) - \frac{M_f}{2} \left(1 + \frac{\mathfrak{q}^2}{4}\right) \mathfrak{q}^2 = M_f \left(1 - \sqrt{1 - \mathfrak{q}^2} - \frac{\mathfrak{q}^2}{2} - \frac{\mathfrak{q}^4}{8}\right) \geq M_f \frac{\mathfrak{q}^6}{16},$$

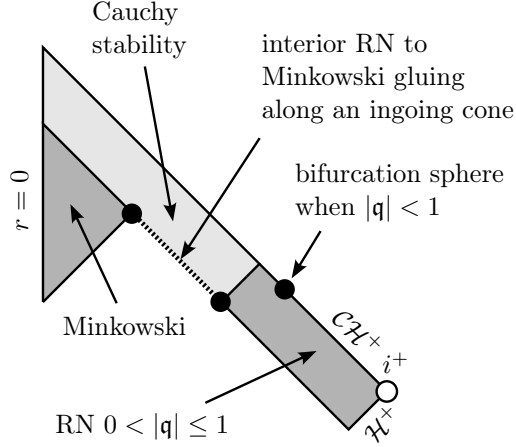


Figure 14: Penrose diagram depicting the proof of Corollary 3.

where in the last step we used the Taylor expansion of $\sqrt{1-q^2}$ around $q = 0$. The rest of the proof is now analogous to Corollary 2 and can be read off from Fig. 14. We note that an isometric copy of the Reissner–Nordström exterior can be attached to the past of \mathcal{H}^+ in Fig. 14. \square

A An isolated extremal horizon with nearby trapped surfaces

In this appendix we show that, in the context of the dominant energy condition, there is no local mechanism forcing a stationary extremal Killing horizon to have no trapped surfaces “just inside” of the horizon. We also refer back to Section 1.4.6.

Proposition A.1. *There exists a C^∞ spherically symmetric spacetime (\mathcal{M}^4, g) with a complete null hypersurface $H \subset \mathcal{M}$ and a Killing vector field T with the following properties. The Killing field T is spherically symmetric, timelike in $I^-(H)$, spacelike in $I^+(H)$, null and tangent along H , where it also satisfies $\nabla_T T = 0$, i.e., its integral curves are affinely parametrized null generators of H . Furthermore, (\mathcal{M}, g) contains no antitrapped symmetry spheres, i.e., $\partial_{ur} < 0$, and satisfies the dominant energy condition. Therefore, H is an extremal Killing horizon and $I^+(H)$ is foliated by trapped symmetry spheres.*

We recall that a spacetime (\mathcal{M}, g) satisfies the *dominant energy condition* if for all future directed causal vectors $X \in T\mathcal{M}$, $-G(\cdot, X)^\sharp$ is future directed causal or zero. Here G denotes the Einstein tensor of g ,

$$G(g) \doteq \text{Ric}(g) - \frac{1}{2}R(g)g.$$

Proof. The spacetime is given by the spherically symmetric ansatz

$$\begin{aligned} \mathcal{M} &= \mathcal{Q} \times S^2 \\ g &= g_{\mathcal{Q}} + r^2 g_{S^2}, \end{aligned}$$

where

$$\mathcal{Q} = \{(t, u) \in \mathbb{R}^2 : t \in \mathbb{R}, -\varepsilon < u < \varepsilon\}$$

for ε to be chosen later, and $r = r(u)$. Let $f = f(u)$ and set

$$g_{\mathcal{Q}} = f dt^2 - 2 dt du.$$

The vector field $\underline{L} = \partial_u$ is geodesic and null and we declare it to be future directed. The Killing vector field $T = \partial_t$ satisfies $g(T, T) = f$. Letting $f(u) = u^2 F(u)$ for a smooth function $F(u)$ makes $H = \{u = 0\}$ an extremal Killing horizon and ∂_t is future directed where it is causal. The conjugate null vector to \underline{L} is $L = \partial_t + \frac{1}{2}f\partial_u$ such that $g(\underline{L}, L) = -1$. The symmetry spheres $S_{t_0, u_0} = \{t = t_0\} \cap \{u = u_0\}$ are trapped if

$$\begin{aligned} Lr &< 0 \\ \underline{L}r &< 0, \end{aligned}$$

which can be more simply written as

$$\begin{aligned} f(u)r'(u) &< 0 \\ r'(u) &< 0. \end{aligned}$$

From this we see that $r'(u) < 0$ implies no antitrapped spheres of symmetry and $f(u) < 0$ for $u < 0$ and $f(u) > 0$ for $u > 0$ implies the symmetry spheres to the past (respectively, future) of H are untrapped (respectively, trapped). This also makes T timelike to the past of H . Since we require $f(u) = u^2 F(u)$ but also that f changes sign, we in fact have $f(u) = u^3 \tilde{F}(u)$.

We will now see which restrictions on f , r , and ε enforce the dominant energy condition. The Einstein tensor of g is given by

$$G = -\theta g_{\mathcal{Q}} - \frac{2r''}{r} du^2 + \zeta r^2 g_{S^2}, \quad (\text{A.1})$$

where

$$\theta \doteq \frac{1 + (r')^2 f + r f' r' + 2 f r r''}{r^2}, \quad \zeta \doteq -\frac{1}{2} f'' - \frac{r'}{r} f' - \frac{r''}{r} f.$$

For $f(u) = u^3 \tilde{F}(u)$ and $r(u)$ fixed and $\varepsilon > 0$ sufficiently small, we have $\theta(u) > 0$ and $|\zeta(u)| \ll \theta(u)$ for $|u| < \varepsilon$.

Let X be a future causal vector, that is

$$g_{\mathcal{Q}}(X, X) + r^2 g_{S^2}(X, X) \leq 0, \quad g_{\mathcal{Q}}(\underline{L} + L, X) < 0. \quad (\text{A.2})$$

To show that $-G(\cdot, X)^\sharp$ is causal or zero, it suffices to show that

$$g_{\mu\nu} G^\mu{}_\rho G^\nu{}_\sigma X^\rho X^\sigma \leq 0. \quad (\text{A.3})$$

To simplify the calculation, we assume r'' vanishes identically and then the left-hand side of (A.3), using (A.1) and (A.2), can be estimated as

$$g_{\mu\nu} G^\mu{}_\rho G^\nu{}_\sigma X^\rho X^\sigma = \theta^2 g_{\mathcal{Q}}(X, X) + \zeta^2 r^2 g_{S^2}(X, X) \leq (\zeta^2 - \theta^2) r^2 g_{S^2}(X, X).$$

Since $\zeta^2 - \theta^2 \leq 0$, this proves that $-G(\cdot, X)^\sharp$ is causal. To show that $-G(\cdot, X)^\sharp$ is future directed we compute using (A.2)

$$g(\underline{L} + L, -G(\cdot, X)^\sharp) = -G(\underline{L} + L, X) = \theta g_{\mathcal{Q}}(\underline{L} + L, X) < 0.$$

Finally, an explicit example of a metric satisfying all of our conditions is

$$g = u^3 dt^2 - 2 dt du + (1 - u)^2 g_{S^2}. \quad \square$$

Remark A.1. Extremal Reissner–Nordström has $f(u) \sim -u^2$. One might say that an extremal horizon constructed in the above manner with $f(u)$ vanishing faster than u^2 is a *degenerate extremal horizon*.

B General trapped and antitrapped surfaces in spherically symmetric spacetimes

In this appendix we infer the absence of nonspherically symmetric trapped or antitrapped surfaces from the absence of spherically symmetric trapped or antitrapped surfaces.

Our definition of trapped surface is completely standard, see Definition B.1 below. (Note that we assume trapped surfaces to be closed and strictly trapped.) Our definition of antitrapped is as in [Chr93; Kom13], i.e., an antitrapped surface is closed and past weakly outer trapped, see Definition B.2 below.

Proposition B.1. *Let (\mathcal{M}^4, g) be a spherically symmetric spacetime as defined in Section 2.1. Then there are no trapped surfaces contained in the sets*

$$A \doteq \{p \in \mathcal{M} : \partial_u r \geq 0\}, \quad (\text{B.1})$$

$$B \doteq \{p \in \mathcal{M} : \partial_v r \geq 0\}. \quad (\text{B.2})$$

Remark B.1. Note that there could be trapped surfaces contained in $A \cup B$. There might also be trapped surfaces which merely intersect A or B .

Proposition B.2. *Let $(\mathcal{M}^4, g, F, A, \phi)$ be a spherically symmetric spacetime arising as the maximal future globally hyperbolic development from one-ended asymptotically flat Cauchy data for the EMCSF system with no antitrapped spheres of symmetry as in [Kom13]. Then:*

1. *If S is a trapped surface in \mathcal{M} , then $S \cap J^-(\mathcal{I}^+) = \emptyset$.*
2. *\mathcal{M} does not contain any antitrapped surfaces.*

Remark B.2. Under stronger assumptions on \mathcal{I}^+ , the first part of the previous proposition would follow from a classical result of Hawking [Haw72; HE73, Proposition 9.2.1].

For the proofs, we recall some facts from Lorentzian geometry [Gal00]. Let H be a null hypersurface in a spacetime (\mathcal{M}^4, g) , i.e., H is a 3-dimensional submanifold of \mathcal{M} and admits a future-directed normal vector field L which is null and whose integral curves can be reparametrized to be null geodesics. We say that L is a (future-directed) null generator of H .

The second fundamental form of H with respect to L is given by

$$B^L(X, Y) = g(\nabla_X L, Y) \quad (\text{B.3})$$

for $X, Y \in TH$. If e_1 and e_2 are an orthonormal pair of spacelike vectors at $p \in H$, we define the null expansion of H with respect to L by

$$\theta^L = B^L(e_1, e_1) + B^L(e_2, e_2) \quad (\text{B.4})$$

at p , and this definition is independent of the pair e_1 and e_2 . If \tilde{L} is another future-directed null generator of H , then there is a positive function f on H such that $\tilde{L} = fL$. In this case, we have

$$\theta^{\tilde{L}} = f\theta^L. \quad (\text{B.5})$$

Lemma B.1 (Comparison principle for null hypersurfaces). *Let H_1 and H_2 be null hypersurfaces in (\mathcal{M}^4, g) , with H_1 to the future of H_2 and generated by L_1 and L_2 , respectively. If H_1 and H_2 are tangent at a point p , and $L_1(p) = L_2(p)$, then*

$$\theta_{H_1}^{L_1}(p) \geq \theta_{H_2}^{L_2}(p). \quad (\text{B.6})$$

Proof. By (B.5), it suffices to prove (B.6) with respect to some choice of null generators of H_1 and H_2 which agree at p . Let (t, x, y, z) be normal coordinates for g based at p so that ∂_t is future-directed and $\{\frac{1}{2}(\partial_t + \partial_x), \partial_y, \partial_z\}$ spans $T_p H_1 = T_p H_2$. We introduce approximate null coordinates $u = t - x$ and $v = t + x$, so that

$$\partial_u = \frac{1}{2}(\partial_t - \partial_x), \quad \partial_v = \frac{1}{2}(\partial_t + \partial_x).$$

Note that ∂_u and ∂_v are only guaranteed to be null at p .

By the implicit function theorem, there exist functions $f_1(v, y, z)$ and $f_2(v, y, z)$ defined near p , so that, upon defining

$$\zeta_1(u, v, y, z) \doteq f_1(v, y, z) - u, \quad \zeta_2(u, v, y, z) \doteq f_2(v, y, z) - u,$$

we have $H_i = \{\zeta_i = 0\}$ for $i = 1, 2$. Note that $f_1(p) = f_2(p) = 0$ and that p is a critical point for f_1 and f_2 . The vector fields $Z_i = \text{grad } \zeta_i$ are null on H_i and define their future-directed null generators. In particular, we have $Z_1(p) = Z_2(p) = \partial_v|_p$.

We first show that $f_1 \geq f_2$ near p . If a point $q = (u, v, y, z)$ lies to the past of H_1 , then $\zeta_1(q) \geq 0$. If $q \in H_2$, then $\zeta_2(q) = 0$, so combining these inequalities yields

$$f_1(v, y, z) = \zeta_1(q) + u \geq \zeta_2(q) + u = f_2(v, y, z),$$

as claimed.

We now show that

$$B_{H_1}^{Z_1}(\partial_y, \partial_y)(p) \geq B_{H_2}^{Z_2}(\partial_y, \partial_y)(p), \quad (\text{B.7})$$

the corresponding statement and proof for ∂_z being the same. By (B.4) this will complete the proof. Since $f_1 \geq f_2$ near p , p is a local minimum for $f_1 - f_2$. It follows that

$$\partial_y^2(f_1 - f_2)(p) \geq 0 \quad (\text{B.8})$$

by the second derivative test. Since we are working in a normal coordinate system,

$$B_{H_i}^{Z_i}(\partial_y, \partial_y)(p) = g(\nabla_{\partial_y} \nabla \zeta_i, \partial_y)(p) = \partial_y^2 f_i(p),$$

whence (B.8) proves (B.7), which completes the proof. \square

Definition B.1. A closed spacelike 2-surface S in a spacetime (\mathcal{M}^4, g) is always the intersection of two locally defined null hypersurfaces. We say that S is *trapped* if both of these hypersurfaces have negative future null expansion along S .

Proof of Proposition B.1. We show that there is no trapped surface $S \subset B$. The argument for $S \subset A$ is analogous after noting that $A \cap \Gamma = \emptyset$ by our definition of spherical symmetry and convention for u .

Let $S \subset \{\partial_v r \geq 0\}$ be a closed 2-surface. Let $\pi : \mathcal{M} \rightarrow \mathcal{Q}$ be the projection of the spherically symmetric spacetime to its Penrose diagram. Then $\pi(S)$ is a compact subset of \mathcal{Q} and hence u attains a minimum u_0 on $\pi(S)$.

Therefore, there exists a symmetry sphere S_{u_0, v_0} on which $\partial_v r \geq 0$ such that S lies to the future of C_{u_0} and is tangent to this cone at a point $p \in S_{u_0, v_0}$. Note that $p \notin \Gamma$ because C_{u_0} is not regular there. The condition $\partial_v r \geq 0$ means C_{u_0} has nonnegative future expansion. By Lemma B.1, one of the two null hypersurfaces emanating from S also has nonnegative future expansion, so S is not trapped. \square

Definition B.2. Let (\mathcal{M}^4, g) be a spacetime satisfying the hypotheses of Proposition B.2. A closed spacelike 2-surface S which bounds a compact spacelike hypersurface Ω is said to be *antitrapped* if its future-directed inward null expansion is nonnegative. Here the (locally defined) inward null hypersurface H_{in} emanating from S is chosen to be the one which smoothly extends the boundary of the causal past of Ω .

Proof of Proposition B.2. 1. Since $r \rightarrow \infty$ at \mathcal{I}^+ [Kom13], Raychaudhuri's equation (2.11) implies $\partial_v r > 0$ in $J^-(\mathcal{I}^+)$. Let S be a closed 2-surface such that $S \cap J^-(\mathcal{I}^+) \neq \emptyset$. Let $\pi : \mathcal{M} \rightarrow \mathcal{Q}$ be the projection to the Penrose diagram. Then u attains a minimum u_0 on $\pi(S)$. By the causal properties of $J^-(\mathcal{I}^+)$, there exists a symmetry sphere $S_{u_0, v_0} \subset J^-(\mathcal{I}^+)$ such that S lies to the future of C_{u_0} and is tangent to the cone at $p \in S_{u_0, v_0}$. Arguing as in the proof of Proposition B.1, we see that one of the null hypersurfaces emanating from S has positive future expansion, so S is not trapped.

2. Let $\pi : \mathcal{M} \rightarrow \mathcal{Q}$ be again the projection. Then v attains a maximum v_0 on $\pi(S)$ and again there exists a non-central symmetry sphere S_{u_0, v_0} such that $\partial_u r(u_0, v_0) < 0$, S lies to the past of C_{v_0} , and is tangent to the cone at a point $p \in S_{u_0, v_0}$. Now C_{v_0} is tangent to H_{in} at p and lies to the future, so by Lemma B.1, H_{in} has negative null expansion at p . Therefore, S is not antitrapped. \square

References

- [AL22] X. An and Z. F. Lim. “Trapped surface formation for spherically symmetric Einstein-Maxwell-charged scalar field system with double null foliation”. *Ann. Henri Poincaré* 23.9 (2022), pp. 3159–3190.
- [And14] H. Andréasson. “Black hole formation from a complete regular past for Vlasov matter”. *XVIIIth ICMF*. World Sci. Publ., Hackensack, NJ, 2014, pp. 365–372.
- [Ang16] Y. Angelopoulos. “Global spherically symmetric solutions of non-linear wave equations with null condition on extremal Reissner-Nordström spacetimes”. *Int. Math. Res. Not. IMRN* 11 (2016), pp. 3279–3355.
- [AAG20] Y. Angelopoulos, S. Aretakis, and D. Gajic. “Nonlinear scalar perturbations of extremal Reissner-Nordström spacetimes”. *Ann. PDE* 6.2 (2020), Paper No. 12, 124.
- [Ape22] M. A. Apetroaie. “Instability of gravitational and electromagnetic perturbations of extremal Reissner-Nordström spacetime” (2022). arXiv: 2211.09182.

- [Are11a] S. Aretakis. “Stability and instability of extreme Reissner-Nordström black hole spacetimes for linear scalar perturbations I”. *Comm. Math. Phys.* 307.1 (2011), pp. 17–63.
- [Are11b] S. Aretakis. “Stability and instability of extreme Reissner-Nordström black hole spacetimes for linear scalar perturbations II”. *Ann. Henri Poincaré* 12.8 (2011), pp. 1491–1538.
- [Are15] S. Aretakis. “Horizon instability of extremal black holes”. *Adv. Theor. Math. Phys.* 19.3 (2015), pp. 507–530.
- [Are17] S. Aretakis. “The characteristic gluing problem and conservation laws for the wave equation on null hypersurfaces”. *Ann. PDE* 3.1 (2017), Paper No. 3, 56.
- [ACR21a] S. Aretakis, S. Czimek, and I. Rodnianski. “The characteristic gluing problem for the Einstein equations and applications” (2021). arXiv: 2107.02441.
- [ACR21b] S. Aretakis, S. Czimek, and I. Rodnianski. “The characteristic gluing problem for the Einstein vacuum equations. Linear and non-linear analysis” (2021). arXiv: 2107.02449.
- [ACR21c] S. Aretakis, S. Czimek, and I. Rodnianski. “Characteristic gluing to the Kerr family and application to spacelike gluing” (2021). arXiv: 2107.02456.
- [BCH73] J. M. Bardeen, B. Carter, and S. W. Hawking. “The four laws of black hole mechanics”. *Comm. Math. Phys.* 31 (1973), pp. 161–170.
- [Boo16] I. Booth. “Evolutions from extremality”. *Phys. Rev. D* 93.8 (2016), pp. 084005, 15.
- [BF08] I. Booth and S. Fairhurst. “Extremality conditions for isolated and dynamical horizons”. *Phys. Rev. D* 77.8 (2008), p. 084005.
- [Bor33] K. Borsuk. “Drei Sätze über die n-dimensionale euklidische Sphäre”. ger. *Fundamenta Mathematicae* 20.1 (1933), pp. 177–190.
- [Bou73] D. G. Boulware. “Naked singularities, thin shells, and the Reissner-Nordström metric”. *Phys. Rev. D* 8.8 (1973), p. 2363.
- [Cho93] M. W. Choptuik. “Universality and scaling in gravitational collapse of a massless scalar field”. *Phys. Rev. Lett.* 70.1 (1993), p. 9.
- [Cho09] Y. Choquet-Bruhat. *General relativity and the Einstein equations*. Oxford Mathematical Monographs. Oxford University Press, Oxford, 2009, pp. xxvi+785.
- [CG69] Y. Choquet-Bruhat and R. Geroch. “Global aspects of the Cauchy problem in general relativity”. *Comm. Math. Phys.* 14 (1969), pp. 329–335.
- [Chr70] D. Christodoulou. “Reversible and irreversible transformations in black-hole physics”. *Phys. Rev. Lett.* 25.22 (1970), p. 1596.
- [Chr91] D. Christodoulou. “The formation of black holes and singularities in spherically symmetric gravitational collapse”. *Comm. Pure Appl. Math.* 44.3 (1991), pp. 339–373.
- [Chr93] D. Christodoulou. “Bounded variation solutions of the spherically symmetric Einstein-scalar field equations”. *Comm. Pure Appl. Math.* 46.8 (1993), pp. 1131–1220.
- [Chr99] D. Christodoulou. “The instability of naked singularities in the gravitational collapse of a scalar field”. *Ann. of Math. (2)* 149.1 (1999), pp. 183–217.
- [Chr09] D. Christodoulou. *The formation of black holes in general relativity*. EMS Monographs in Mathematics. European Mathematical Society (EMS), Zürich, 2009, pp. x+589.
- [CRT06] P. T. Chruściel, H. S. Reall, and P. Tod. “On Israel-Wilson-Perjés black holes”. *Classical Quantum Gravity* 23.7 (2006), pp. 2519–2540.
- [CIP21] F. Corelli, T. Ikeda, and P. Pani. “Challenging cosmic censorship in Einstein-Maxwell-scalar theory with numerically simulated gedanken experiments”. *Phys. Rev. D* 104.8 (2021), p. 084069.
- [CS06] J. Corvino and R. M. Schoen. “On the asymptotics for the vacuum Einstein constraint equations”. *J. Differential Geom.* 73.2 (2006), pp. 185–217.
- [CR22] S. Czimek and I. Rodnianski. “Obstruction-free gluing for the Einstein equations” (2022). arXiv: 2210.09663.

- [Daf03] M. Dafermos. “Stability and instability of the Cauchy horizon for the spherically symmetric Einstein-Maxwell-scalar field equations”. *Ann. of Math. (2)* 158.3 (2003), pp. 875–928.
- [Daf09] M. Dafermos. “Black hole formation from a complete regular past”. *Comm. Math. Phys.* 289.2 (2009), pp. 579–596.
- [DHR] M. Dafermos, G. Holzegel, and I. Rodnianski. “The linear stability of the Schwarzschild solution to gravitational perturbations”. *Acta Math.* 222.1 (2019), pp. 1–214.
- [DHRT] M. Dafermos, G. Holzegel, I. Rodnianski, and M. Taylor. “The non-linear stability of the Schwarzschild family of black holes” (2021). arXiv: 2104.08222.
- [DI67] V. De la Cruz and W. Israel. “Gravitational bounce”. *Il Nuovo Cimento A (1965-1970)* 51.3 (1967), pp. 744–760.
- [FH79] C. J. Farrugia and P. Hajicek. “The third law of black hole mechanics: a counterexample”. *Comm. Math. Phys.* 68.3 (1979), pp. 291–299.
- [Fou52] Y. Fourès-Bruhat. “Théorème d’existence pour certains systèmes d’équations aux dérivées partielles non linéaires”. *Acta Math.* 88 (1952), pp. 141–225.
- [Gaj17a] D. Gajic. “Linear waves in the interior of extremal black holes I”. *Comm. Math. Phys.* 353.2 (2017), pp. 717–770.
- [Gaj17b] D. Gajic. “Linear waves in the interior of extremal black holes II”. *Ann. Henri Poincaré* 18.12 (2017), pp. 4005–4081.
- [GL19] D. Gajic and J. Luk. “The interior of dynamical extremal black holes in spherical symmetry”. *Pure Appl. Anal.* 1.2 (2019), pp. 263–326.
- [Gal00] G. J. Galloway. “Maximum principles for null hypersurfaces and null splitting theorems”. *Ann. Henri Poincaré* 1.3 (2000), pp. 543–567.
- [GHHP83] G. W. Gibbons, S. W. Hawking, G. T. Horowitz, and M. J. Perry. “Positive mass theorems for black holes”. *Communications in Mathematical Physics* 88 (1983), pp. 295–308.
- [GM07] C. Gundlach and J. M. Martín-García. “Critical Phenomena in Gravitational Collapse”. *Living Rev. Relativ.* 10.1 (2007).
- [Haw71] S. W. Hawking. “Gravitational radiation from colliding black holes”. *Phys. Rev. Lett.* 26.21 (1971), p. 1344.
- [Haw72] S. W. Hawking. “Black holes in general relativity”. *Comm. Math. Phys.* 25 (1972), pp. 152–166.
- [Haw75] S. W. Hawking. “Particle creation by black holes”. *Comm. Math. Phys.* 43.3 (1975), pp. 199–220.
- [HE73] S. W. Hawking and G. F. R. Ellis. *The large scale structure of space-time*. Cambridge Monographs on Mathematical Physics, No. 1. Cambridge University Press, London-New York, 1973, pp. xi+391.
- [Isr86] W. Israel. “Third law of black-hole dynamics: a formulation and proof”. *Phys. Rev. Lett.* 57.4 (1986), pp. 397–399.
- [Isr92] W. Israel. “Thermodynamics and internal dynamics of black holes: Some recent developments”. *Black hole physics*. Springer, 1992, pp. 147–183.
- [KV21] C. Kehle and M. Van de Moortel. “Strong Cosmic Censorship in the presence of matter: the decisive effect of horizon oscillations on the black hole interior geometry” (2021). arXiv: 2105.04604.
- [Keh22] L. M. A. Kehrberger. “The case against smooth null infinity I: Heuristics and counter-examples”. *Ann. Henri Poincaré* 23.3 (2022), pp. 829–921.
- [Kom13] J. Kommemi. “The global structure of spherically symmetric charged scalar field spacetimes”. *Comm. Math. Phys.* 323.1 (2013), pp. 35–106.
- [Kuc68] K. Kuchař. “Charged shells in general relativity and their gravitational collapse”. *Czechoslovak Journal of Physics B* 18.4 (1968), pp. 435–463.

- [LM20] J. Li and H. Mei. “A construction of collapsing spacetimes in vacuum”. *Comm. Math. Phys.* 378.2 (2020), pp. 1343–1389.
- [LY15] J. Li and P. Yu. “Construction of Cauchy data of vacuum Einstein field equations evolving to black holes”. *Ann. of Math. (2)* 181.2 (2015), pp. 699–768.
- [LMRT13] J. Lucietti, K. Murata, H. S. Reall, and N. Tanahashi. “On the horizon instability of an extreme Reissner-Nordström black hole”. *J. High Energy Phys.* 3 (2013), 035, front matter+43.
- [Luk12] J. Luk. “On the local existence for the characteristic initial value problem in general relativity”. *Int. Math. Res. Not. IMRN* 20 (2012), pp. 4625–4678.
- [LO19] J. Luk and S.-J. Oh. “Strong cosmic censorship in spherical symmetry for two-ended asymptotically flat initial data I. The interior of the black hole region”. *Ann. of Math. (2)* 190.1 (2019), pp. 1–111.
- [LOY18] J. Luk, S.-J. Oh, and S. Yang. “Solutions to the Einstein-scalar-field system in spherical symmetry with large bounded variation norms”. *Ann. PDE* 4.1 (2018), Paper No. 3, 59.
- [MRT13] K. Murata, H. S. Reall, and N. Tanahashi. “What happens at the horizon (s) of an extreme black hole?” *Classical Quantum Gravity* 30.23 (2013), p. 235007.
- [Ner26] W. Nernst. *The New Heat Theorem: Its foundations in theory and experiment*. EP Dutton, 1926.
- [Nir01] L. Nirenberg. *Topics in nonlinear functional analysis*. Vol. 6. Courant Lecture Notes in Mathematics. New York University, Courant Institute of Mathematical Sciences, New York; American Mathematical Society, Providence, RI, 2001, pp. xii+145.
- [OS39] J. R. Oppenheimer and H. Snyder. “On continued gravitational contraction”. *Phys. Rev. (2)* 56.5 (1939), pp. 455–459.
- [Ori91] A. Ori. “Charged null fluid and the weak energy condition”. *Classical Quantum Gravity* 8.8 (1991), pp. 1559–1575.
- [Pró83] M. Prószyński. “Thin charged shells and the violation of the third law of black hole mechanics”. *Gen. Relativity Gravitation* 15.5 (1983), pp. 403–415.
- [SI80] B. T. Sullivan and W. Israel. “The third law of black hole mechanics: What is it?” *Phys. Lett. A* 79.5-6 (1980), pp. 371–372.
- [TA14] J. M. Torres and M. Alcubierre. “Gravitational collapse of charged scalar fields”. *Gen. Relativity Gravitation* 46.9 (2014), pp. 1–36.
- [Van18] M. Van de Moortel. “Stability and instability of the sub-extremal Reissner-Nordström black hole interior for the Einstein-Maxwell-Klein-Gordon equations in spherical symmetry”. *Comm. Math. Phys.* 360.1 (2018), pp. 103–168.
- [Van19] M. Van de Moortel. “The breakdown of weak null singularities inside black holes” (2019). *Duke Math. J.* (to appear). arXiv: 1912.10890.
- [Wal84] R. M. Wald. *General relativity*. University of Chicago Press, Chicago, IL, 1984, pp. xiii+491.
- [Wal97] R. M. Wald. “The Nernst theorem and black hole thermodynamics”. *Phys. Rev. D* 56.10 (1997), p. 6467.
- [Wal01] R. M. Wald. “The Thermodynamics of Black Holes”. *Living Rev. in Rel.* 4.6 (2001).